Sources of atmospheric volatile organic compounds during the Salt Lake regional Smoke, Ozone and Aerosol Study (SAMOZA) 2022

Emily M. Cope[1], Damien T. Ketcherside[1], Lixu Jin[1], Lu Tan[1], Marc Mansfield[2,3], Colleen Jones[3], Seth Lyman[2,3], Dan Jaffe[4,5], and Lu Hu[1]

[1]Department of Chemistry and Biochemistry, University of Montana, Missoula, MT, USA.

[2]Department of Chemistry and Biochemistry, Utah State University, Logan, UT, USA.

[3]Bingham Research Center, Utah State University, Vernal, UT, USA.

[4]School of STEM, University of Washington Bothell, Bothell, WA, USA.

[5]Department of Atmospheric Sciences, University of Washington, Seattle, WA, USA.

Corresponding author: Emily Cope (emily.cope@umontana.edu)

Key Points:

- Methanol and ethanol dominated the total measured VOC abundance while isoprene dominated total OH reactivity from VOCs in Salt Lake City
- Traffic and solvent use are roughly equivalent contributors to anthropogenic VOC emissions in Salt Lake City during SAMOZA
- Ozone production was limited by VOCs in Salt Lake City in summer 2022

Abstract

We present measurements of volatile organic compounds (VOCs) and other trace gases taken in Salt Lake City, Utah in August and September 2022. As part of the Salt Lake regional Smoke, Ozone and Aerosol Study (SAMOZA), 35 VOCs were measured with two methods: a proton-transfer-reaction time-of-flight mass spectrometer (PTR-ToF-MS) and 2,4-dinitrophenylhydrazine (DNPH) cartridges analyzed by high-performance liquid chromatography (HPLC). Over two months, the total measured VOCs averaged 32 ± 24 ppb (mean ± standard deviation) with the hourly maximum at 141 ppb, and the total calculated OH reactivity averaged 3.7 ± 3.0 s^{-1} (maximum at 20.7 s^{-1}). Among them, methanol and ethanol were the most abundant VOCs, making up 42% of the ambient mixing ratio. Isoprene and monoterpenes contributed 25% of the OH reactivity from VOCs, while formaldehyde and acetaldehyde made up another 30%. The positive matrix factorization analysis showed 5 major sources of VOCs, with 32% of abundance being attributed to secondary production/biogenic sources, followed by 29% as traffic, 15% from industrial solvent use, and the rest from personal care products (15%) and biomass burning (10%). Moderate smoke-impacted days on average elevated various hazardous air pollutants (HAPs) by 45-217% compared to smoke-free days. The ratio of OH reactivity from NO_x to that from VOCs showed that ozone production was mostly VOC-limited throughout the campaign, consistent with our modeling study. VOCs and NO_x both showed increased OH reactivity due to smoke influence. NO_x featured increased reactivity on weekdays compared to weekends, an effect not shown for VOC reactivity during SAMOZA.

1 Introduction

Salt Lake City (SLC) metropolitan area in Wasatch Front, Utah, United States is a non-attainment area for the 2015 National Ambient Air Quality Standards (NAAQS) for ozone (i.e., the 3-year average of the annual fourth-highest daily maximum 8-hour average ozone [MDA8] not exceeding 70 ppb). With a total population of 2.13 million people, all 5 counties in the Northern and South Wasatch Fronts were designated either marginal or moderate non-attainment regions (https://www3.epa.gov/airquality/greenbook/anayo_ut.html). Ground-level ozone is a photochemical product of nitrogen oxides (NO_x = NO + NO_2) and volatile organic compounds (VOCs) in the presence of sunlight and has serious impacts on the health of the public, ecosystem, and crops (Felzer et al., 2011; Nuvolone et al., 2018). However, its sources are complex, including the local mix of anthropogenic origins of NO_x and VOCs, uncontrolled sources such as biogenic or biomass burning, and long-range transport. Thus, ozone control policy could vary city by city and require detailed knowledge of sources of precursors, particularly for VOCs due to their complex origin in the urban atmosphere. Here we present observations of a suite of VOCs and other trace gases made during the Salt Lake regional Smoke, Ozone and Aerosol Study (SAMOZA) in August – September of 2022 and interpret the data in terms of their origins and implications for ozone photochemistry in this region.

VOCs are emitted from a wide variety of sources in the urban atmosphere. Within cities, common anthropogenic VOCs, such as aromatic compounds, often come from cars/trucks and industry, with some contribution from long-range transport depending on the season and lifetime of the compound (Hu et al. 2015a). Although vehicle design has been improved to reduce VOC emissions, on-road emissions are still an important contributor to US urban VOCs (Warneke et al., 2012). In the Intermountain West, emissions from oil and natural gas development have been reported to enhance anthropogenic VOCs, including benzene and toluene, thus contributing to

high ozone abundance, for example, in the Colorado Front Range during spring and summer (Abeleira et al., 2017). In Utah, the oil and gas production activities are mostly concentrated in the east side of the State, i.e., the Uintah basin, and thus are thought to have no or little impact on SLC (Womack et al., 2019). However, there are various petroleum industries including oil refineries located in the Salt Lake City metropolitan area (Bhardwaj et al., 2021). Industrial sites near urban areas can emit VOCs that are carried downwind to cities and contribute to pollution (Gilman et al., 2013). In addition, Salt Lake City houses a variety of other manufacturing and power plants in and around the city, from tubing and other materials manufacturing to aluminum processing to power plants and refineries, which all emit VOCs that affect the area (https://deq.utah.gov/air-quality/2017-statewide-emissions-inventories). Previous studies reported abundances of methanol up to 80 ppb and acetaldehyde up to 7 ppb during wintertime (Baasandorj et al., 2018), and formaldehyde reaching over 30 ppb throughout the year (Bhardwaj et al., 2021) in SLC. These high levels of VOCs were thought to, at least to a certain extent, be linked to such point sources from petroleum or other industries.

The use of solvents, also called volatile chemical products (VCPs), has become an increasingly important source of VOCs, particularly as vehicle emissions have decreased in the past few decades (McDonald et al., 2018). These VCPs also come from many of the products that are used on a daily basis, such as D5 siloxane from personal care products and monoterpenes from fragrances. Buildings themselves can emit VOCs from the offgassing of paint and wood products, though the fluxes of such emissions are highly uncertain (Gkatzelis et al., 2021). Such paints and coatings, personal care products, and cleaning products are thought to contribute the most to VCP emissions, which could account for more than 50% of anthropogenic VOC contribution to ozone formation in certain US cities (Coggon et al., 2020; Seltzer et al., 2021).

The relative contribution of VCPs to anthropogenic VOC emissions is likely to vary in different urban areas, in part due to the large differences in population density. For example, limited observational evidence suggested VCP emissions contributed to ~40% of anthropogenic VOC emissions in Boulder, CO, up to half in Los Angeles, CA, but ~80% in New York City, NY, while the remainder was often attributed to mobile emissions (60%, 50%, and 20%) in the above 3 urban areas (Gkatzelis et al., 2021; McDonald et al., 2018). It is broadly consistent with the recent bottom-up emission inventory suggesting that VCPs have become a dominant source of anthropogenic VOCs in many US urban areas (Seltzer et al., 2021).

In Salt Lake City, the 2017 Northern Wasatch Front VOC and NOx Inventories, which is based on the EPA's 2017 National Emission Inventory (NEI), estimate that 44% of summertime VOC emissions come from VCP/solvent uses, while only 23% of emissions come from onroad sources (https://home.chpc.utah.edu/~u0864163/OZONE_public/NWF-SMOKE-Summary-Report.html). On an annual basis, the updated 2020 National Emissions Inventory from the EPA also shows the importance of solvent use, with an estimated 27% of anthropogenic emissions coming from solvent use, compared to 25% from onroad sources. The remaining anthropogenic emissions come from other fuel combustion, such as aircraft and residential sources, as well as industrial processes and agriculture.

Emissions of biogenic VOCs (BVOCs), including isoprene and monoterpenes (Folberth et al., 2006; Guenther et al., 2012), are known to be important contributors to ozone formation when interacting with urban NO_x sources because of their reactivity and emission fluxes, which are often higher than those of typical anthropogenic VOCs (NRC, 1991). Isoprene concentration is thought to be low in the western US compared to the east coast and southeast US, while

emissions of monoterpenes from needleleaf trees are supposed to be the dominant BVOCs in the western US. However, uncertainties of these biogenic emissions are high, likely on the order of a factor of 2 or higher (Sakulyanontvittaya et al., 2008). In addition, recent studies also suggested that isoprene and monoterpenes in the urban atmosphere may in part reflect anthropogenic emissions from VCPs or instrument interferences (Coggon et al., 2021; Gkatzelis et al., 2021; Hu et al., 2015b; Peng et al., 2022). BVOC emissions are affected greatly by environmental parameters including temperature and sunlight and are dependent on tree species or plant functional types (Churkina et al., 2017; Gu et al., 2021; Ma et al., 2022). Salt Lake City boasts around 85,000 trees within its limits (https://www.slc.gov/parks/urban-forestry/), which have many benefits for the residents, but can also contribute to BVOC levels in the city. BVOCs can be transported from upwind forests, which have been found to affect nocturnal chemistry and contribute to high-ozone events the following day (Millet et al., 2016). These BVOC emissions can complicate source attribution, as many compounds are co-emitted from anthropogenic and biogenic sources including OVOCs such as methanol and acetone.

Smoke from wildland fires is another natural source that increases VOC levels and ozone production in urban areas, especially in the western U.S. (Jaffe et al., 2020). Wildfires have been suggested to be the second largest VOC source in the western US, though the uncertainty of their emissions is also high and is thought to be on the order of a factor of 2-3 at least for this region (Jin et al., 2023). The species emitted by wildfires depend on the biomass types and burn conditions, among other factors (Gilman et al., 2015; Sekimoto et al., 2018) and can include gases like formaldehyde and methanol, as well as NO_x (Liu et al., 2017; Permar et al., 2021). As gases are transported from the fire, they undergo oxidation reactions via sunlight or chemical species like OH radicals. The distance a smoke plume travels will affect the level of oxidation it undergoes and will therefore dictate the composition of the plume as it reaches an urban site, however in general smoke from wildland fires tends to be VOC-rich and NO_x-poor (Liang et al., 2022; Permar et al., 2023). Thus each smoke event could be unique because of this dependence on the location of emitted VOCs and those that reach the urban site. Once wildfire smoke reaches a city, it mixes with urban emissions, often NO_x-rich, to degrade air quality and increase ozone production. In many cases, ozone increases due to increased VOC levels (Dreessen et al., 2016; Jaffe et al., 2013; Lill et al., 2022; Permar et al., 2023). Salt Lake City was seen to have elevated ozone concentrations due to wildfires upwind of the region in the summer of 2015 (Gong et al., 2017; Horel et al., 2016). The chemical regime within the urban atmosphere may shift as gas concentrations change, often transitioning from VOC-limited to transitional or NO_x-limited scenarios as VOC levels rise without a corresponding increase in NO_x levels (Liang et al., 2022; Rickly et al., 2023).

The SAMOZA field campaign aimed to better understand the factors leading to the high levels of ozone in Salt Lake City by exploring its sources and how atmospheric composition is affected by wildfire smoke (Jaffe et al., 2024). In this work, we report the abundance of 35 VOCs measured during the campaign and investigate their sources and atmospheric impact in SLC. The abundance, composition, and reactivity of total and speciated VOCs in SLC are presented. Their sources are then characterized using positive matrix factorization (PMF) and corroborated by source tracer analysis. The impact of wildfire smoke is assessed for VOC abundance and reactivity. Finally, the implications for photochemistry leading to ozone production in SLC are explored. Further analysis and results from the campaign have also been recently published. Jaffe et al. (2024) provides a general overview of the key results of the campaign. Ninneman et al. (2023) presents results from a photochemical box model constrained

by observations from the campaign to describe ozone formation in the region. Lee and Jaffe (2024) uses a generalized additive model to investigate the impact of wildfire smoke on ozone concentrations in SLC over 16 years, including the measurement period of SAMOZA.

2 Materials and Methods

2.1 Measurement Site and Meteorological Data

Measurements for the SAMOZA study were conducted in Salt Lake City, Utah from August 1 to September 30, 2022. The campaign measurements took place at the Utah Department of Environmental Quality Technical Support Center (UDAQ UTC), located approximately ~3 km east of the Salt Lake City International Airport at 40.778° N, -111.946° W. UDAQ UTC sits on the northeast corner within a multi-agency business complex, surrounded by the residential neighborhood to its north and east, and is 5 km away from SLC downtown. Being at the intersection of 3 major Interstate Highways (~0.3 km east of I-215, 1.2 km north of I-80, and 3 km west of I-15,) UDAQ UTC is expected to be a high NO_x and receptor site of diverse urban sources.

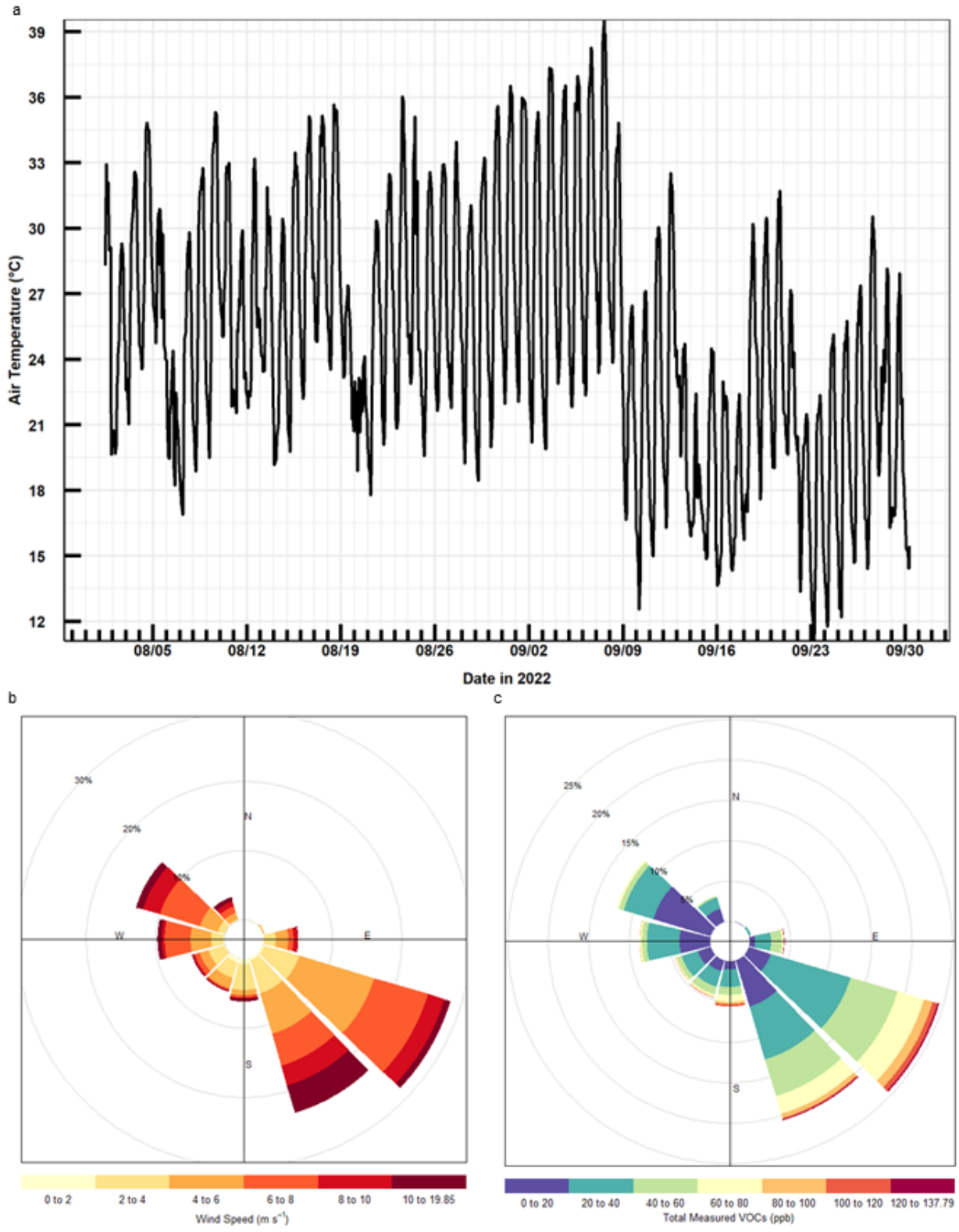

Figure 1. Meteorological conditions at the UDAQ UTC site during the SAMOZA field

campaign (August 1-September 30, 2022). a) air temperature (°C); b) Wind direction as a function of wind speed (m/s); and c) Wind direction as a function of total measured VOCs (ppb).

Figure 1 shows the air temperature measured at UDAQ UTC during the SAMOZA campaign, as well as wind rose plots showing the wind direction as a function of wind speed and total measured VOCs. Temperature data was collected by the UDAQ using an electronic thin film air temperature sensor. Wind direction and speed were measured with 2D-ultrasonic anemometer transducers. All meteorological instruments were situated on a tower with a height of 10 meters above the roof at UDAQ UTC (Utah DAQ, 2022). The air temperature was warmer for the first part of the campaign through September 9th (27 ± 5°C; mean ± standard deviation). Most days during the first period reached a daily highest temperature of over 30°C, with the daily lowest temperature often being over 20°C (21 ± 2°C). From September 9th until the end of the campaign, daily average temperatures dropped to 21 ± 5°C. The daily low temperature during this period dropped by nearly 6°C compared to the previous period (15 ± 2°C), with the high temperature only exceeding 30°C six days out of the 21-day period. Wind came mostly from the southeast at night, while during daytime wind direction tended to shift to the west or northwest during SAMOZA (Figure S1). The highest wind speed seen was 19 m/s, while the average was around 6 m/s.

2.2 VOC Measurements by PTR-ToF-MS

Ambient VOCs were measured using proton-transfer-reaction time-of-flight mass spectrometry (PTR-ToF-MS 4000, Ionicon Analytik GmbH, Innsbruck, Austria). The conditions in the drift tube were held constant during the campaign at 3.00 mbar, 60°C, and 815 V, which made for an electric field (E/N) of 135 Townsend (Td). The PTR was located on the second floor of UDAQ UTC. The ~10 m long sampling inlet was made from perfluoroalkoxy (PFA, 1/4'' OD) tubing and was situated on the roof of the building, ~ 20 m above ground level. The air was subsampled by the PTR-ToF-MS through ~100 cm of 1/16" (1.59 mm) OD polyetheretherketone (PEEK) tubing maintained at 60°C. Ions from m/z 19 to 400 were measured once every minute. Instrument background was taken approximately every 2½ hours by measuring VOC-free air generated by ambient air passing through a heated catalytic converter (375°C, platinum beads, 1 wt% Pt: Sigma Aldrich).

In this work, we include 27 VOC species measured by PTR-ToF-MS in the analysis, which are listed in the supplement (Table S1). Among them, calibrations were performed for 22 species in two compressed gas standard cylinders following previously established procedures (stated accuracy 5% at ~1 ppmv; Apel-Riemer Environmental, Inc., Miami, FL, USA; Permar et al., 2021; Selimovic et al., 2022). One standard gas cylinder with 10 species was used every other day during the campaign. A second standard gas cylinder containing 15 species was used every other day for the first three weeks of the campaign. For isomers calibrated at the same m/z (i.e., methyl vinyl ketone and methacrolein at m/z 71.049; ethylbenzene and o-xylene at m/z 107.086; 1,2,4- and 1,3,5-trimethylbenzene at m/z 121.101), a weighted average sensitivity was found using corresponding isomeric contributions per previous urban studies. Six-point calibrations were performed by diluting the gas standards with the VOC-free air described above, at a range between 1 and 7 ppb. Only calibrations with an r^2 above 0.998 and those sensitivities for the same species that did not vary by 10% of the mean during the campaign were used. In addition, D5 Siloxane was calibrated with a gas standard in June 2022 before the campaign (stated accuracy 5% at ~1 ppm; Apel-Riemer Environmental, Inc., Miami, FL) using dynamic dilution

as described above. From quadrature addition of individual errors including calibrations and mass flow controllers in the instrument, uncertainty for these species is estimated to be <15%.

Formaldehyde was calibrated after the campaign using a gas standard cylinder (stated accuracy 5% at ~2 ppm; Airgas USA LLC, Plumsteadville, PA, USA) diluted with a zero-air generator (7000 Zero Air Generator, Environics, Tolland, CT, USA). Gases were mixed in a Liquid Calibration Unit (Ionicon Analytik GmbH, Innsbruck, Austria) and water vapor was introduced in the sample to derive the dependence of instrument sensitivity on changing humidity. Formic acid and acetic acid were calibrated before the campaign using liquid standards evaporated and diluted with zero-air in the same Liquid Calibration Unit. Humidity dependence of instrument sensitivity was considered as well. Uncertainty for these species is estimated at 40%, with the major source of error being the humidity dependence.

Sensitivity for maleic anhydride was estimated using the method by Sekimoto et al. (2017) from its molecular dipole moment and polarizability. The procedure for the calculation was further refined in our previous work (Permar et al., 2021). The uncertainty for this species is estimated to be 50%.

Mass spectra were first analyzed with Ionicon's PTR-Viewer software (Version 3.4, Ionicon Analytik). One-minute mass calibrations performed during the campaign were refined using 4 ion peaks: m/z 29.997 [NO^+], 59.049 [$C_3H_6OH^+$], 203.943 [$C_6H_4IH^+$], and 330.848 [$C_6H_4I_2H^+$]. Ion counts for each peak in the list were calculated by the PTR-Viewer software through a baseline correction as well as a correction for mass discrimination in the time-of-flight mass spectrometer. The calculated ion counts were then exported for further processing in R. Instrument background was linearly interpolated and subtracted from the data. Each ion was then normalized to the primary ion [H_3O^+] and water cluster ion [$(H_2O)H_3O^+$]. Normalized counts were converted to mixing ratios using the calibrations or theoretical sensitivities described above.

2.3 Additional Measurements

In addition to the standard UDAQ measurements of CO at UTC (Teledyne API T300U, San Diego, CA, USA), we made concurrent CO measurements using gas chromatography (GC) with a reducing compound photometer (Peak Performer 1 RCP; Peak Laboratories LLC., Mountain View, CA, USA). In this technique, CO eluting from the GC column passes directly into a heated mercuric oxide bed, resulting in liberated mercury vapor, which is subsequently measured via UV light absorption in the photometer cell. Compressed ultra-high purity (UHP) air was used as the carrier gas. Multi-point calibrations are carried out before and after the campaign by dilution of a ppm-level standard (Scott Specialty Gases, USA; stated accuracy ± 2%) into UHP air. The detection limit for CO is 300 ppt and the time resolution of the data was 3 minutes. The comparisons of two CO measurements, SAMOZA CO and UDAQ CO, show a high correlation during the campaign (r^2 = 0.86 and slope = 1.15 with hourly data), with SAMOZA data being systematically higher most of the time. This is likely due to the instrument background drift issue of the regulatory UDAQ CO measurements. It has little policy implication given that SLC CO concentrations rarely exceed the national ambient standard, but it does affect the following analysis. Thus for the rest of the work, we use the CO measurements made by the GC RCP based instrument.

Carbonyl samples were collected three times per day using 2,4-dinitrophenylhydrazine (DNPH) cartridges using automatic sampling trays. Cartridges were sampled for three hours with an air flow around 1 L min^{-1}. High-performance liquid chromatography (HPLC) was used to

analyze collected samples and quantify the concentrations of 13 different carbonyl species. Samples were kept refrigerated after collection. They were eluted within 14 days of measurement and further analyzed within 30 days. Calibrations were performed with a commercial standard mixture (M-1004; AccuStandard) each day samples were analyzed. Of those carbonyl species measured, 5 overlapped with measurements from the PTR-ToF-MS. In these cases, the PTR-ToF-MS data was prioritized due to the higher temporal resolution. When data from the two methods was compared, the PTR-ToF-MS showed lower concentrations of acetone than DNPH-HPLC, but higher concentrations of formaldehyde, acetaldehyde, and methyl ethyl ketone (Jaffe et al., 2024). The rest of the 8 carbonyl species (all aldehydes) were added to the following analysis and are listed in the supplement (Table S1). The species were used in statistical analysis of VOC composition as well as OH reactivity.

Hourly measurements of $PM_{2.5}$, ozone, and NO_x provided by UDAQ were also used in our analysis. Ozone was measured with a Teledyne T400 instrument. Nitrogen dioxide (NO_2) and nitric oxide (NO) were measured using gas phase chemiluminescence (Teledyne API T200U, San Diego, CA, USA). $PM_{2.5}$ was measured with two Synchronized Hybrid Ambient Real-Time Particulate Monitors (Thermo Environmental 5030i and Thermo Environmental 2025i, Waltham, MA, USA).

2.4 Determination of Smoke-influenced Days

Each day during the campaign was classified as either being smoke-influenced or smoke-free based on two criteria. The first was the presence of overhead smoke as determined by the National Oceanic and Atmospheric Administration Hazard Mapping System Fire and Smoke Product (https://www.ospo.noaa.gov/Products/land/hms.html). It was not used as the only criterion for smoke-influenced days because the presence of overhead smoke does not necessarily indicate that smoke is present at the surface. A second criterion for the concentration of $PM_{2.5}$ at the site was added to ensure the smoke was present at the surface. The mean (6.23 µg m^{-3}) and standard deviation (1.85 µg m^{-3}) were found for days without any indication of overhead smoke. Days that showed overhead smoke and had a $PM_{2.5}$ concentration one standard deviation above the non-smoke influenced mean were classified as being smoke-influenced. Using these criteria, 10 days out of the campaign were described as smoke-influenced, while 51 days were described as smoke-free. As shown in Section 3.2, our VOC analysis still shows some smoke influence in those 51 days. More details on the smoke day identification during SAMOZA can be found at Jaffe et al. (2024).

2.5 Positive Matrix Factorization Analysis

We performed a positive matrix factorization (PMF) analysis using 26 of the 27 VOCs measured with PTR-ToF-MS for detailed source attribution on the 51 days without the influence of smoke. Dimethyl sulfide was excluded from the analysis due to the majority of the data being below the detection limit. The results were then compared with the traditional approaches including known source tracers and tracer:tracer ratios for qualitative verifications. PMF analysis does not allow for gaps in the data, thus any time that did not have measurements for all 26 species was excluded from the model. The analysis is based on the following mathematical model of the data. Let C_{tc} represent the concentration of compound c at time t. We assume there are a number of sources or factors, each one possessing its own temporally-uniform concentration signature. Let X_{sc} represent the mole fraction of compound c in source s. As a mole fraction, X_{sc} is unitless and its sum over compounds is 1: $\Sigma_c X_{sc} = 1$. We assume that T_{ts}

concentration units of source s are present at time t, so that $T_{ts}X_{sc}$ represents the concentration of compound c derived from source s at time t. Summing over all sources yields the modeled concentration of compound c at time t:

$$C'_{tc} = \sum_s T_{ts}X_{sc} \#(1)$$

The prime is used to distinguish modeled and measured concentrations. In our work, T_{sc}, C_{tc}, and C'_{tc} are in ppb units. Note that this equation represents a matrix product. Therefore, the procedure consists of determining two initially unknown matrices T_{ts} and X_{sc} that optimize the fit between C_{tc} and C'_{tc} (Paatero & Tapper, 1994). Because negative values of T_{ts} and X_{sc} are physically excluded, the optimization must be carried out subject to the constraints $T_{ts} \geq 0$ and $X_{sc} \geq 0$.

We used the EPA Positive Matrix Factorization 5.0 tool (Norris et al., 2014) to perform the optimization, with 20 independent runs with unique random seeds to verify that the analysis converged consistently to the same solution. The number of factors is entered into the model by the user. One criterion used to determine the appropriate solution was the ratio of Q (goodness-of-fit parameter calculated with all points) to $Q_{expected}$ (goodness-of-fit parameter excluding points for which the residual divided by uncertainty is greater than 4), or Q/Qexpected. Increasing the number of factors should decrease $Q/Q_{expected}$ closer to a value of 1 as the error and/or variability in factor profiles is better accounted for (Ulbrich et al., 2009). The number of factors was changed between 3 and 9, with a steady decrease in $Q/Q_{expected}$ as the number increased. However, the solution with 5 factors and $Q/Q_{expected}$ value of 2.56 was chosen for this analysis due to unreasonable factor splitting as the number increased above 5. This solution doesn't account for as much error but can be physically interpreted with comparison to meteorological and concentration data.

Uncertainty for each species is given by the user, in the same units as the concentration. This analysis used uncertainties obtained by multiplying each hourly concentration by its percent uncertainty stated in section 2.2. The EPA's PMF model includes the option to label a species as "Strong," "Weak," or "Bad," to further manipulate the uncertainty and therefore how much a species will contribute to the solution. All species are automatically given the Strong label, which indicates that the uncertainty supplied by the user will be used. Those species with the Weak label will have their uncertainties multiplied by 3, so that they have less effect on the solution the model reaches. Any species with the Bad label will be excluded altogether (Norris et al. 2014). Before running the model, the signal to noise ratio (S/N) is calculated by the program for each species. Signal is assigned as 0 for species with greater uncertainty than concentration, and for all other species the signal is the difference between the concentration and uncertainty. The S/N is then calculated as the sum of the signal for each data point divided by the number of data points (Norris et al. 2014).

All 26 species showed S/N greater than 0.5 and were therefore left with the default Strong label. After running the model, the uncertainty-scaled residuals (residual divided by uncertainty) were evaluated for each species. For those species with residuals outside of the range between -3 and 3, the EPA's standard for a good fit of their model, the observed concentration was compared with the predicted concentration. Any of those species with large residuals and with an r^2 value less than 0.6 were labelled as Weak, and the model ran again with the new uncertainties. From these evaluations, 5 of the 26 included species (furfurals, hexanone, methyl furfurals, acetonitrile, and formic acid) were labeled as Weak, while the remaining 21 kept the default label of Strong. Error was estimated using the model's bootstrap method. The model creates a new dataset by randomly selecting portions of the data until the length of the original dataset is

reached. The PMF analysis is then performed again with the new dataset, and each new factor is mapped against the factor from the original dataset that it has the highest correlation with, above a threshold defined by the user (Norris et al., 2014). For this analysis, a minimum correlation value of 0.72 yielded no unmapped factors. Factor 2 mapped to its original factor for 52% of the runs, and all other factors mapped to the original more than 90%.

3 Results and Discussion

3.1 Overview: VOC Abundance, Composition, and Reactivity in SLC

Figure 1 shows the meteorological data and Figure 2 shows the time series for ozone, CO, NO_x, and selected VOCs measured during SAMOZA. August-September 2022 at the SLC airport was slightly warmer (~2°C) than the decadal mean and was a relatively modest smoke year with 10 out of 61 days identified as smoke-influenced days during SMAOZA (Jaffe et al., 2024). As mentioned above, the average daily air temperature was ~10°C higher in the first ~2/3 of the SAMOZA period than the last 1/3 of days, reflecting the hot/dry summer to cool/wet autumn seasonal transition in SLC starting around September 9, 2022. Interestingly, five out of the 10 smoke days occurred in September when the air temperature was cooler, including the four of the smokiest days (9^{th}-12^{th} September 2022) that reached the highest daily mean $PM_{2.5}$ of 25.3-33.8 ug/m^3 during SAMOZA (Jaffe et al., 2024). It is likely that those smoke days were influenced by large fires burning in other western states and transported to SLC. Our VOC analysis shown later also suggests the smoke was indeed aged during SAMOZA (Section 3.3). Ozone concentrations averaged 37 ± 19 ppb (average ± standard deviation), with hourly peaks above 70 ppb on 22 days, and five MDA8 exceedance days (8/4, 8/9, 9/3, 9/7, 9/11). The corresponding averaged NO_x was 16 ± 13 ppb at the UDAQ UTC site, comparable to the level in other non-attainment urban areas in the western US (i.e., May-September averaged ~15 ppb across 20 west urban sites in Jaffe et al. 2022).

Over the two months of SAMOZA, the total measured VOC mixing ratio averages 36 ± 24 ppb (or 82 ± 55 ppbC). Wind rose plots in Figure S1 show the wind direction separated by day and night. These plots suggest that the highest frequency of wind came from the southeastern direction, which mostly occurred at night (18:00 – 06:00 Mountain Standard Time). This direction was also correlated with the higher mean concentration of VOCs during the campaign compared to the western wind, at 35 ± 26 ppb. As the UDAQ UTC location was situated in the northwestern part of Salt Lake City, southeasterly winds could be influenced by various urban sources in the city. A significant amount of wind also came from the west and northwestern direction, mostly also occurring during daytime when the photochemical loss of VOCs is strong and the atmospheric boundary layer is high. It resulted in a lower total measured VOC abundance (19.4 ± 13 ppb) under such conditions when the site is likely influenced by the industrial sites and Salt Lake City International Airport.

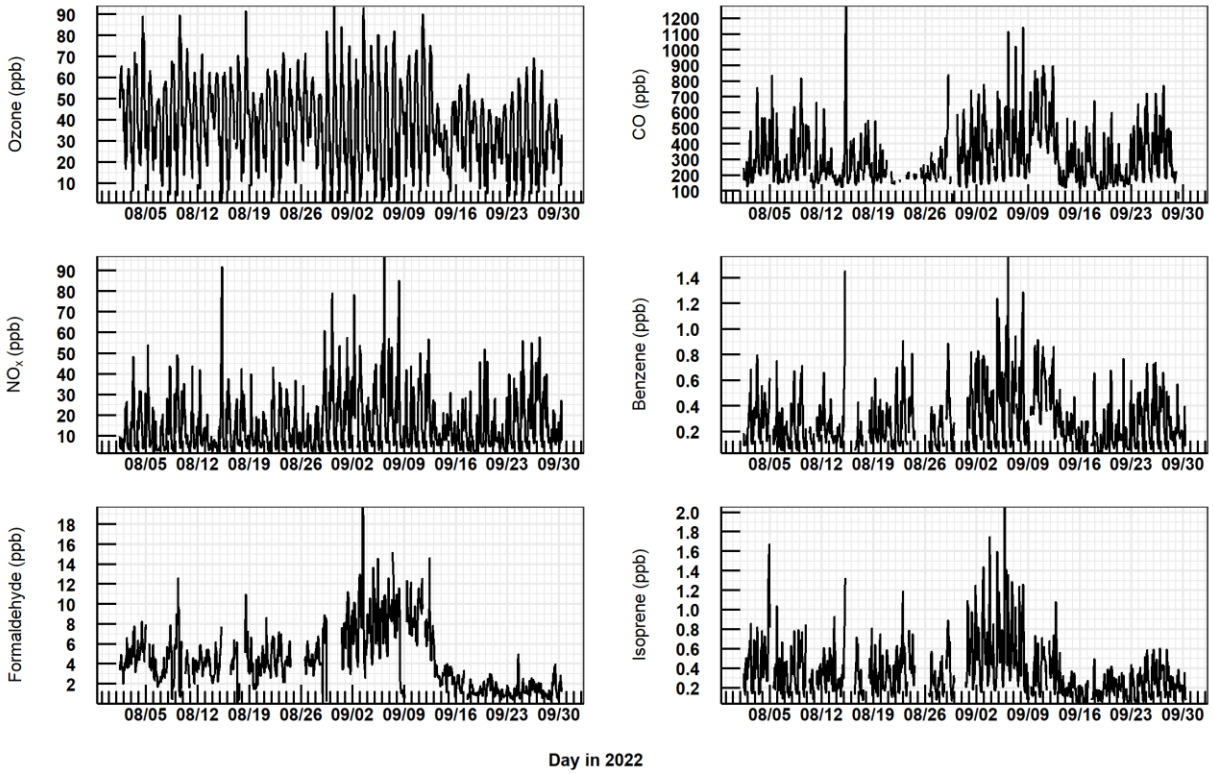

Figure 2. Time series plots for hourly concentrations of ozone, CO, NO_x, and selected VOCs including benzene, formaldehyde, and isoprene between August 1 and September 30, 2022 during the SAMOZA field campaign.

The overall VOC composition during SAMOZA appears to have two distinct distributions likely controlled by air temperature. VOC species mostly driven by primary anthropogenic emissions, such as benzene, toluene, and ethanol, as well as CO and NO_x, do not show significant changes when the air temperature dropped in the middle of September (Figure 2). However, those compounds with biogenic origin or photochemical sources exhibit a similar pattern of decreased concentration by 35-50% starting around September 12th when daily average air temperature was about 10°C lower than the previous period. Isoprene and monoterpenes are examples that are often majorly influenced by biogenic sources, though urban sources or measurement interferences could play a nonnegligible role (Borbon et al., 2023; Coggon et al., 2023; Hu et al., 2015b). Formaldehyde and other species like methyl vinyl ketone and methacrolein (MVK + MACR) with large photochemical productions also show this pattern of decreased concentration with temperature towards the end of the campaign. Most of the mixing ratios for these species (formaldehyde, methyl ethyl ketone [MEK], MVK + MACR, and acetaldehyde) were 35-45% lower compared to the average of the first 2/3 of the period. When the daily average mixing ratio for the VOCs was correlated against the daily average temperature, those secondary and biogenic species showed significantly higher r^2 values (e.g., 0.58 for formaldehyde, 0.64 for isoprene) than the species that did not show decreased temperature after September 9th (e.g., 0.18 for benzene, 0.13 for ethanol), further indicating that temperature played a role in controlling VOCs from biogenic sources or secondary production.

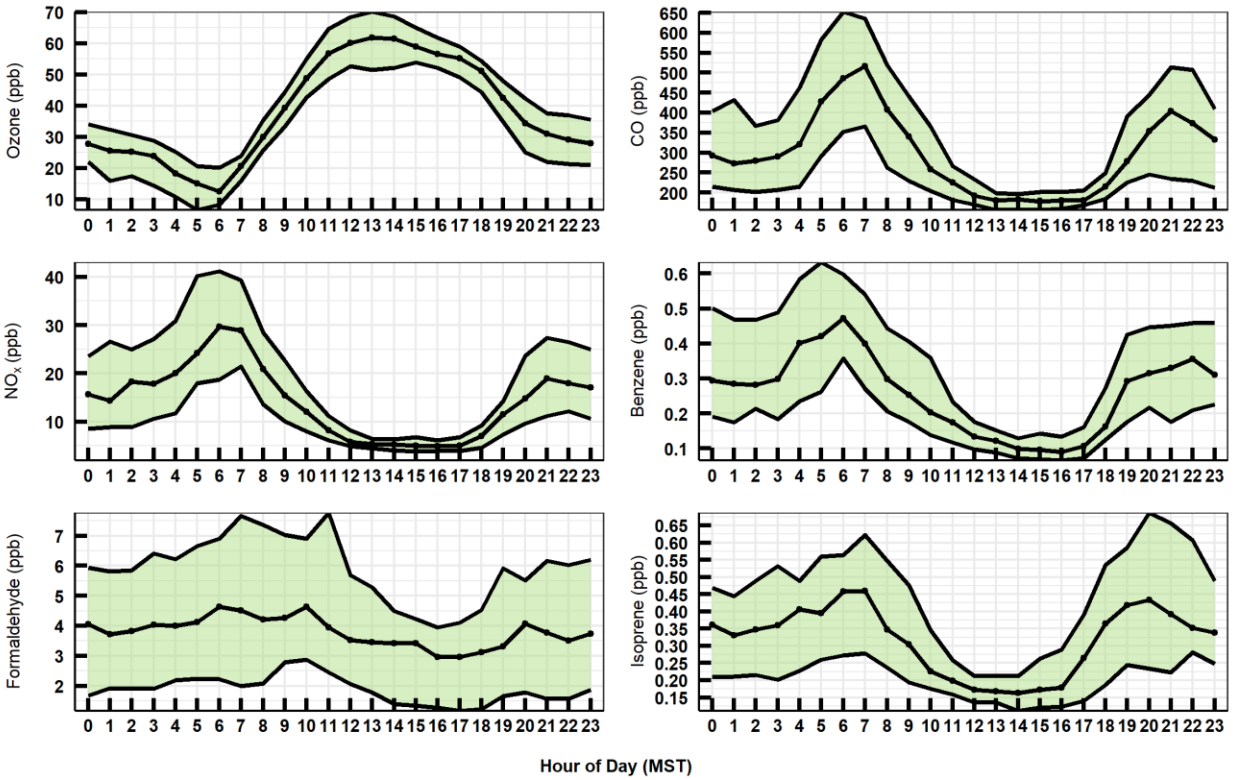

Figure 3. Diurnal variations of ozone, CO, NO_x, benzene, formaldehyde, and isoprene observed during SAMOZA (August 1 to September 30, 2022). The thick middle lines indicate the median mixing ratio, with the shaded areas as 25^{th}-75^{th} percentiles of the observations.

The diurnal patterns for primary anthropogenic VOCs mostly showed a similar pattern, with a large peak in concentration early in the morning (06:00 – 09:00 Mountain Standard Time), rapid decreasing during the day, and then increasing at night (Figure 3). Such diurnal profiles have been widely documented in urban sites (e.g. Bryant et al., 2023; Coggon et al., 2018; de Gouw et al., 2017; Li et al., 2022), reflecting the combined effects of emission strength and atmospheric boundary layer dynamics, while the ratios of nighttime and daytime values are often determined by their lifetimes (de Gouw et al. 2017). The group of C_6-C_{10} aromatic compounds is one such example. These compounds are highly correlated to each other (R^2 ranging from 0.75 to 0.94) and show the same diurnal patterns but have averaged nighttime: daytime ratios (22:00-06:00 / 10:00-18:00) increasing from 2.2 (benzene) to 4.3 (C_{10} aromatics) following the increasing order in their OH rate constants. Oxygenated VOCs, such as formaldehyde, formic acid, and MVK+MACR, had a slight peak in the morning but did not show the same large decrease during the day as in other species. This is due to their sources, either biogenic or photochemical, being enhanced during the day when the solar radiation is strong and temperature is high, even though they may also have primary anthropogenic emissions in urban areas. Isoprene showed a similar diurnal pattern to benzene and CO, which could indicate a strong anthropogenic influence in SLC in addition to biogenic emissions. Later in Section 3.2, we will present a more quantitative analysis of their sources in SLC.

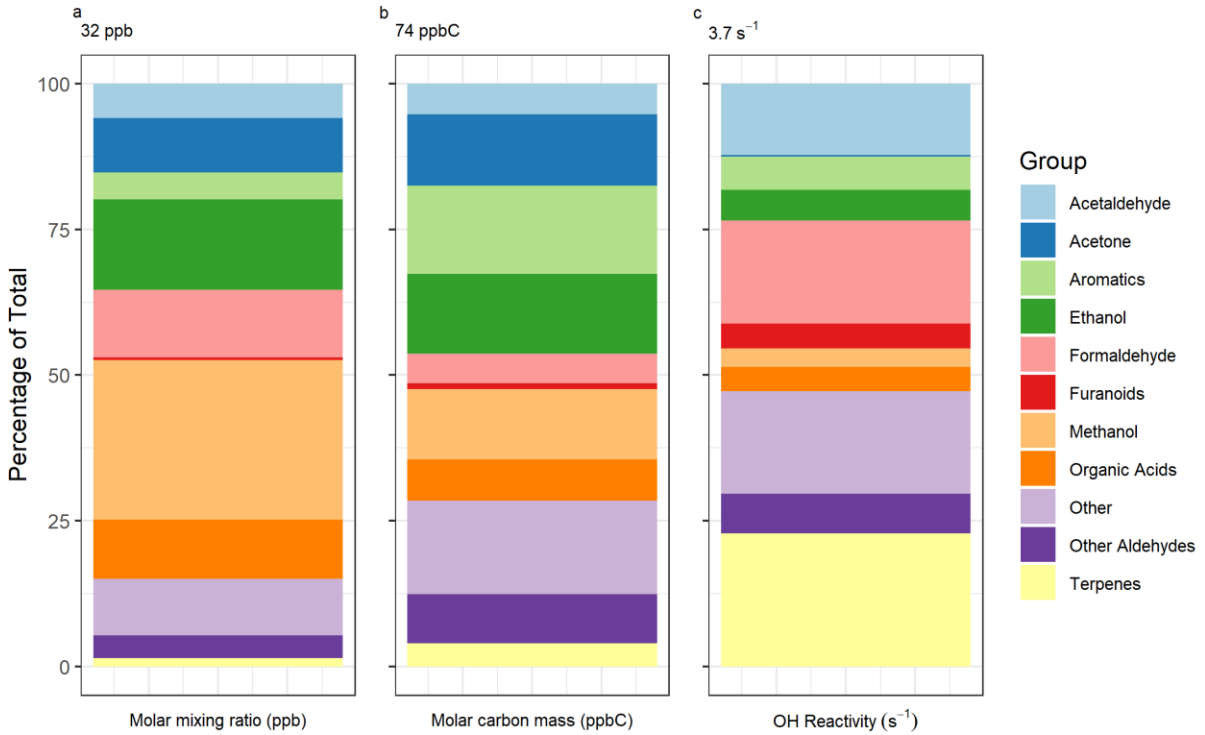

Figure 4. The campaign-averaged contribution of major VOC species/groups to total measured VOCs in SLC during SAMOZA as a) molar mixing ratio in ppb, b) molar carbon mass in ppbC, and c) daytime OH reactivity in s^{-1}. For the VOC groups, Aromatics include benzene, toluene, and C_8, C_9 and C_{10} aromatics; Furanoids include furan, methylfuran, furfural, and methyl furfural; Organic Acids include formic acid and acetic acid; Other includes propyne, acetonitrile, butene, dimethyl sulfide, MVK + MACR, methyl ethyl ketone (MEK), maleic anhydride, hexanone, and D5 siloxane; Other Aldehydes includes the aldehydes measured with DNPH cartridge: acrolein, propionaldehyde, crotonaldehyde, n-butyraldehyde, valeraldehyde, hexaldehyde, benzaldehyde, and m-tolualdehyde; Terpenes include isoprene and monoterpenes. The average values for each metric are shown at the top of the bars. VOC data from 35 species/masses are from both PTR-ToF-MS and DNPH/HPLC measurements. See Table S1 for details.

Figure 4 shows the percent contribution of VOCs for the SAMOZA campaign average, separated into major functional groups and major individual contributors, to overall molar mass (ppb), molar carbon mass (ppbC), and OH reactivity (s^{-1}). Here we integrated the DNPH/HPLC measurements for a more complete list of species; all 8 species are included under the Other Aldehydes category. The total measured VOCs from 35 species/masses averaged 32 ± 24 ppb, with a median of 27 ppb (Interquartile range (IQR) of 27 ppb, and max 141 ppb). This corresponds to 74 ± 57 ppbC (median 58 ppbC, IQR 64 ppbC, and max 345 ppbC).

OH reactivity was calculated for VOCs for Figure 4 as well as for NO_x for later analyses according to the equation

$$OHR = k_{OH+X}[X] \#(2)$$

Where k_{OH+X} is the rate constant for the reaction of species X with the OH radical and [X] is the measured species concentration. Rate constants were taken from Permar et al. 2023, with

additional rate constants not included (propyne, D5 siloxane, and NO_x) found using the NIST chemical kinetics database (https://kinetics.nist.gov/kinetics/). Concentrations for each species were converted to number density in molecules per cm^3 using the field-measured temperature and pressure. The total calculated OHR from measured VOCs averaged 3.7 ± 3.0 s^{-1}, with a median of 2.9 s^{-1} (IQR 2.7 s^{-1} and max 20.7 s^{-1}) for the SAMOZA campaign.

Methanol was the most abundant VOC in SLC in terms of mixing ratio (27% of total measured VOCs), followed by ethanol (16%). This is consistent with other urban areas such as in India (Kalbande et al., 2022) and France (Simon et al., 2023). In contrast, ethanol was found to be the most abundant VOC in Guangzhou, China, followed by methanol (Li et al., 2022). Methanol is thought to have a large biogenic origin even in urban atmospheres (de Gouw et al., 2005; Hu et al., 2011; MacDonald & Fall 1993; Salisbury et al., 2003). Although ethanol can be found in fuel, it has been shown to have significant biogenic sources in the western US (Millet et al., 2012) and has recently been attributed to VCPs in urban areas (McDonald et al., 2018). Also among the most abundant VOCs were acetone (9%), acetic acid and acetaldehyde (both 6%), and formaldehyde (12%).

When weighted by the number of carbons, methanol is not as important a contributor, only accounting for 12% of the total measured VOC carbon. Aromatic compounds saw a large increase in contribution by this metric (5% of total measured VOCs to 15% of total measured VOC carbon). VOCs in the Other category, such as acetonitrile, butenes, and propyne, also saw an increase in contribution in this way (10% total measured VOCs compared to 16% total measured VOC carbon).

In terms of OH reactivity, isoprene and monoterpenes, lumped as Terpenes in Figure 4, were the most abundant (23% of total VOC OH reactivity) despite making up less than 2% of the total mixing ratio due to their rapid reactions with OH radicals. Isoprene has been shown to be a large contributor to VOC OH reactivity in urban regions of South Korea (Sanchez et al., 2021) and Canada (Stroud et al., 2008). In other urban areas, OH reactivity from VOCs has been more largely influenced by aromatics and alkenes from traffic and industrial sources (Gilman et al., 2009) or OVOCs such as carbonyls and alcohols (Hansen et al., 2021). Similarly to the biogenic influence on VOC abundance, Salt Lake City appears to have a large influence from biogenic emissions on daytime photochemistry. Formaldehyde and acetaldehyde were also important contributors to OH reactivity at 18% and 12% of the total, respectively. Furanoids including furan, methyl furans, furfural, and methylfurfurals, were some of the least abundant VOCs by all three metrics (i.e., <1% of total measured VOCs), reflecting their relatively small urban and BB emissions during SAMOZA.

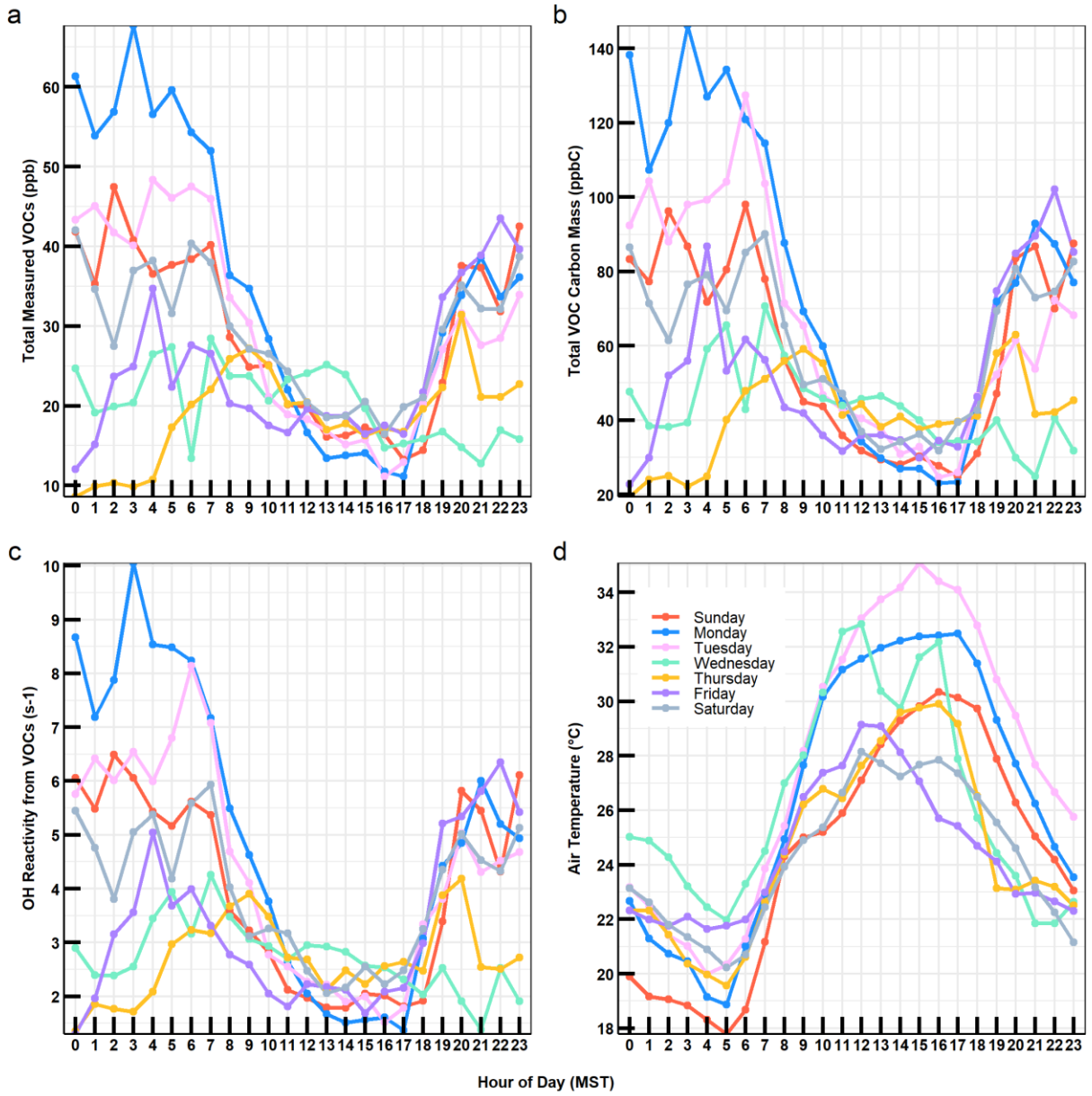

Figure 5. Diurnal patterns for a) the median total measured VOC concentration in ppb, b) the median total ppbC, c) the median total OHR from VOCs in s^{-1}, and d) the median air temperature averaged by day of the week for the 51 smoke-free days over the two-month SAMOZA period. This includes 7 Sundays, 8 Mondays, 9 Tuesdays, 7 Wednesdays, 7 Thursdays, 7 Fridays, and 6 Saturdays.

Figure 5 shows the diurnal pattern for total median VOC concentrations and OH reactivity separated by the days of the week. VOC abundances peak in the evening and early morning and show a large dip in the middle of the day as temperatures rise and the atmospheric boundary layer breaks down. The highest daily concentration of VOCs is present on Mondays and Tuesdays (35 ± 27 ppb vs. 31 ± 24 ppb). Thursdays show the lowest daily VOC concentration (21 ± 18 ppb), with the lowest concentrations observed during the night, not consistent with the pattern of the other days of the week, when the lowest concentrations were

observed between 12:00 and 18:00 MST. The concentration of VOCs is consistent with the patterns of NO_x also measured during SAMOZA (Jaffe et al., 2024). OHR and VOC carbon mass showed similar patterns, with Mondays and Tuesdays being the highest (5.2 ± 4.2 s^{-1} vs. 4.4 ± 3.8 s^{-1}; 80 ± 65 ppbC vs. 67 ± 58 ppbC) and Thursdays being the lowest (3.0 ± 2.6 s^{-1}; 45 ± 39 ppbC). The exact reasons for the patterns of the days of the week are unknown but it may be related to emission patterns and meteorological conditions. Mondays and Tuesdays indeed show higher daytime (06:00 to 18:00 MST) temperatures than the other days, averaging 29 ± 5.1°C compared to 26 ± 5.5°C. However, when plotted against temperature, the median values did not show any clear pattern, so the role of temperature is not well known. When we removed those Mondays and Tuesdays with particularly high values of total measured VOCs to investigate if the pattern was affected by them, as was the case for NO_x in Jaffe et al. (2024), we found such omission made little difference in the diurnal patterns. When examining the weekday vs. weekend difference, we found there are no statistically significant differences in total VOC abundance or OH reactivity (Section 3.4). Future work to include longer periods of observation will help improve statistics and examine if there are meaningful emission differences in the days of the week in SLC.

3.2 Sources of Major VOCs

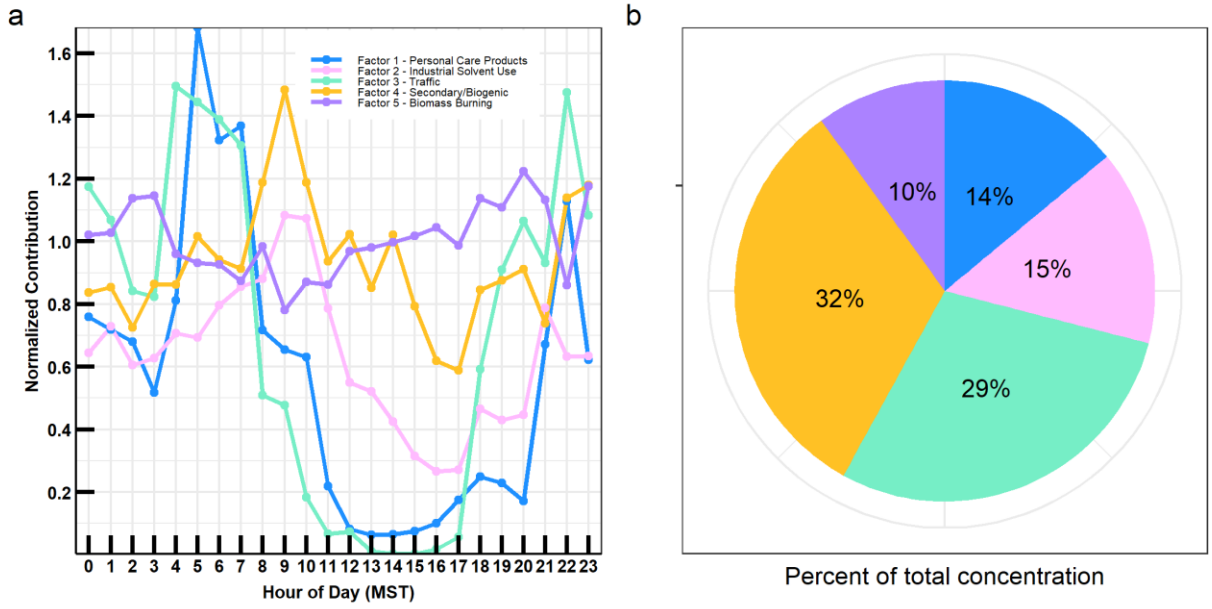

Figure 6. a) Diurnal pattern of median normalized concentration for each factor in the PMF analysis: Factor 1 – Personal Care Products dominated, Factor 2 – Industrial Solvent Use, Factor 3 – Traffic dominated, Factor 4 – Secondary/Biogenic, Factor 5 – Biomass Burning. b) Pie chart showing the percentage of total concentration contributed by each factor.

Here we investigate the main sources of VOCs in SLC using PMF analysis. The identity of the factors was assigned based on features in the time series and correlation with other tracers and meteorological conditions such as temperature and solar radiation. The diurnal patterns of the factors are given in Figure 6a and were also used in identification. The abundance of species within the factor profiles (shown in Figure S2) was used as the final confirmation of the source. Factors 1 and 3 are dominated by Personal Care Products and Traffic sources, respectively. They correlate well with NO_x and CO and have a similar diurnal pattern, with a large dip in the day in the diurnal pattern, discussed previously as an indicator of anthropogenic influence. Notably, there are significant amounts of aromatic compounds attributed to the personal care product factor, and significant amounts of D5 siloxane and monoterpenes attributed to the Traffic factor. Co-emission of these compounds during peak traffic times may explain the difficulty in fully extricating these two sources in PMF (Coggon et al., 2018). Ultimately, Factor 1 was assigned as Personal Care Products dominated due to the high abundance of monoterpenes and low abundance of benzene, and Factor 3 was assigned as Traffic dominated due to high amounts of both benzene and toluene.

Factor 2 is assigned as Industrial Solvent Use due to a similar diurnal pattern to the other anthropogenic factors, albeit with a shallower dip during the day in the diurnal pattern as well as high levels of OVOCs like MEK and formaldehyde. Factor 4 includes species produced in photochemical reactions and emitted by biogenic sources. The diurnal pattern shows no large decrease in concentration during daylight hours likely due to increased chemical reactions and plant activity. This factor also showed a large decrease after September 9 when the air temperature dropped 10°C, reflecting the seasonal reduction in photochemical and plant biological activities. Important species for this factor include formaldehyde, isoprene, and its oxidation products MVK+MACR. Factor 5 is labeled as Biomass Burning due to containing much of the furanoid species and acetonitrile and because it does not have a distinct diurnal pattern, with the median concentration staying similar throughout the day.

The pie chart in Figure 6b shows large contributions from Secondary/Biogenic sources (~32%). According to this model, traffic emissions are still a large contributor to VOCs in SLC at 29% of total abundance. Using only Factors 1, 2, and 3 as primary urban emissions, traffic contributes 50% of the anthropogenic VOCs, while Personal Care Products and Industrial Solvent Use are roughly equal at 25%. Since the latter two factors both fall under the category of VCPs, this means that traffic and VCPs contribute about the same to anthropogenic VOCs in SLC, similar to what was estimated in the 2020 NEI. We note that PMF results shown here, though somewhat quantitative, could be subject to other compounding factors, such as the Personal Care Products and Traffic factors are not able to be fully resolved due to their similar emission patterns.

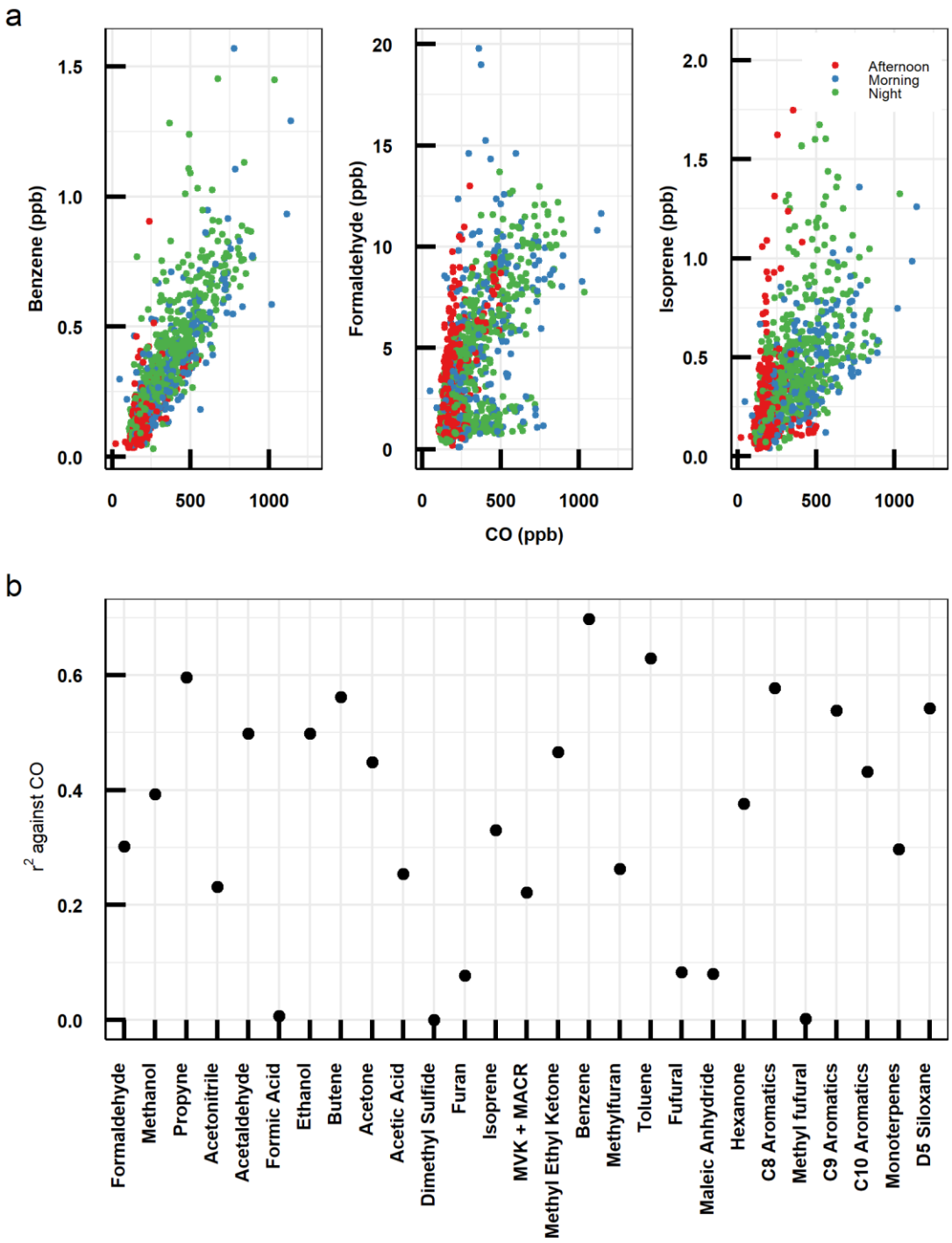

Figure 7. a) Benzene, formaldehyde, and isoprene mixing ratios plotted against observed CO, all in ppb. The data points are colored by the time of day: morning was defined as 06:00-12:00 MST, afternoon was defined as 12:00-18:00 MST, and night was defined as 18:00-06:00 MST. b) The r^2 value for the reduced major axis regression of each VOC against CO measured during SAMOZA.

We further use source tracer analysis to test if it can qualitatively confirm the PMF findings or not, with a particular focus on well-known emission tracers or signatures. Figure 7 shows benzene, formaldehyde, and isoprene correlated with carbon monoxide (CO), a vehicle tracer that is not used in PMF, and colored by time of day. Correlation coefficient values are also given for all 27 VOC species measured by PTR-ToF-MS. Benzene and other aromatic compounds were seen to correlate best with CO (0.70 and 0.63, respectively), with no apparent difference in population based on time of day. Although they can have several anthropogenic sources, aromatic compounds are present in vehicle fuel and known to be co-emitted with CO. Formaldehyde and other compounds with secondary production sources are seen to have two populations and lower correlation with CO, with the highest slopes seen in the afternoon when chemical production is highest. Within the PMF model, 54% of formaldehyde was assigned to the Secondary/Biogenic factor, while the rest was split between the three anthropogenic factors. Isoprene and other biogenic VOCs show a similar low correlation with CO and multiple populations. Slopes were not as clearly separated for these compounds as for formaldehyde. A large amount of isoprene comes from biogenic sources as stated previously, but there are some anthropogenic sources as well (Bryant et al., 2023; Khan et al., 2018; Wagner & Kuttler, 2014). From the PMF analysis, 40% of isoprene was assigned to the Secondary/Biogenic factor, and 50% was mapped to the three anthropogenic factors. When plotted against CO, the Traffic factor showed the highest correlation ($r^2 = 0.58$), while the other anthropogenic factors had lower correlation (0.23 for Personal Care Products and 0.19 for Industrial Solvent Use), and the natural factors had the lowest correlation (<0.01 for Secondary/Biogenic and Biomass Burning). The considerable number of VOCs correlating with CO corroborates the PMF findings that Traffic is an important VOC source in SLC.

The ratio of toluene to benzene is another important emission signature for traffic, biomass burning, and industrial sources. Figure S3 shows the correlation between the two species. The ratio of toluene to benzene in SLC during SAMOZA was 2.02. Ratios higher than 1 are commonly seen in urban settings with significant solvent use in the area, and ratios between 1-10 are commonly seen when traffic is the major VOC source (Zhang et al., 2016). Data here is given for the full two-month campaign. Separating the data by smoke-influenced and smoke-free days did not change the ratio significantly, with values of 2.09 and 2.06, respectively. This ratio also corroborates the assignment of the anthropogenic factors in the PMF model. The Traffic factor had a lower toluene/benzene ratio (1.55) than that of Personal Care Products (2.44) or Solvent Use (2.43).

In addition, isoprene and monoterpenes are known to be emitted from biological processes in plants. Figure S4 shows the correlations of each compound with temperature. Isoprene concentration has a strong increase with temperature, while monoterpenes reach the highest concentration at 22°C with a decrease at higher and lower temperatures. When correlated with CO, colored by temperature, isoprene shows some separation in correlation. Higher temperatures led to a higher slope. Monoterpenes, in contrast, do not show this same separation. This agrees with the PMF analysis, wherein roughly 76% of the concentration of monoterpenes was attributed to the factors for Personal Care Products and Traffic.

D5 Siloxane can be used as a tracer for personal care products (Gkatzelis et al., 2021), but shows similar emission patterns as traffic. In Salt Lake City, we see a strong correlation between D5 and benzene during SAMOZA ($r^2 = 0.72$; Figure S5). They show similar diurnal patterns as well, with peaks early in the morning as traffic begins. The two are not perfectly

correlated, as humans spend much of their time indoors rather than driving, but there is some overlap there, similar to the emission features derived by Coggon et al. (2018). As discussed above, PMF cannot tell such co-emitted features from two different sources, with about 60% of D5 siloxane and 40% of benzene mapped to Traffic, and 20% of each to the Personal Care Products dominated factor. Therefore the PMF results here should be considered semi-quantitative. Future studies including more source tracers or source measurements from mobile platforms can help better understand the the complexity of urban emissions in SLC.

3.3 Impact of Wildfire Smoke

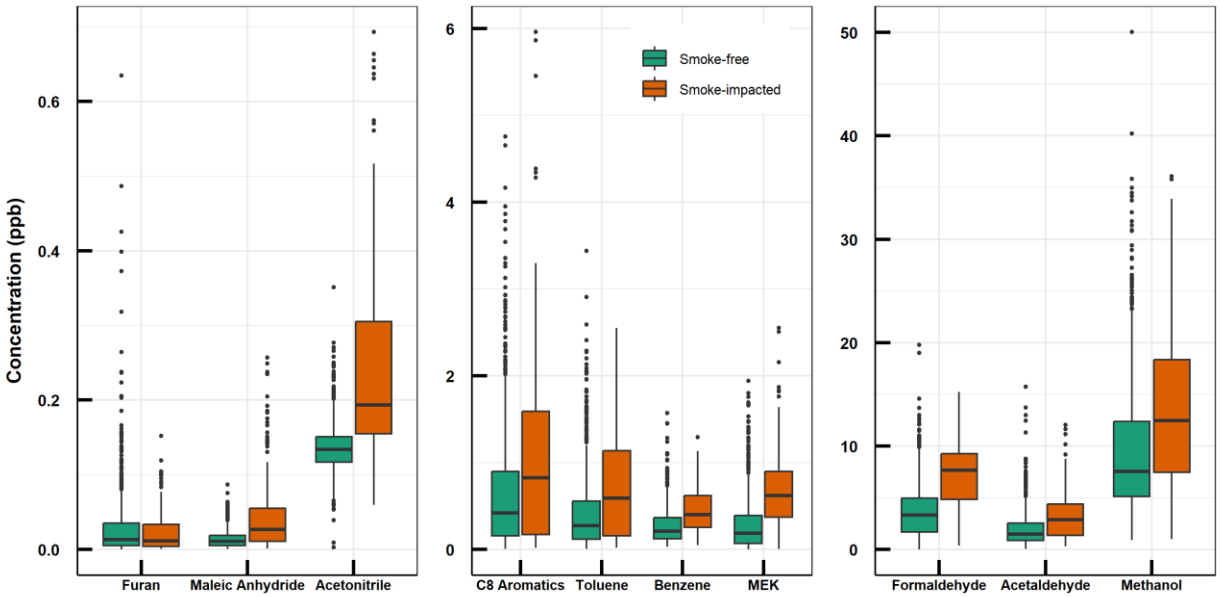

Figure 8. Box and whisker plot showing the concentration of key wildfire-related species (furan, maleic anhydride, and acetonitrile) as well as Hazardous Air Pollutants (HAPs) identified by the EPA (C8 aromatics, toluene, benzene, MEK, acetaldehyde, formaldehyde, and methanol) in ppb. The concentration is shown for the 51 smoke-free days and the 10 smoke-influenced days during SAMOZA.

Figure 8 shows key species on smoke-influenced days and smoke-free days during SAMOZA. The average abundance of total VOCs increased from 33 ± 21 to 50 ± 28 ppb when fire smoke impacted the area. Most individual VOCs (26 out of 35) also show enhancements during smoke-influenced days, with the largest enhancement being present for maleic anhydride and MEK at over 100% increases compared to smoke-free days. Acetonitrile is enhanced by 85% in the presence of smoke. Acetonitrile has been widely used in past studies as a biomass burning tracer, even though it also has a smaller anthropogenic source that is also reflected in our PMF analysis (Huangfu et al., 2021). Furan shows slightly lower concentration on days that are smoke-enhanced, while maleic anhydride shows an enhancement in smoke of 400%. Furan is emitted directly from biomass burning and has a short lifetime (estimated 7 hours assuming OH concentrations of 1.0×10^6 molecules/ cm^3). It reacts rapidly with OH radicals to form oxidation products including maleic anhydride, which has a longer lifetime (estimated 8 days) (Bierbach et

al., 1994, 1995). The high maleic anhydride and low furan levels indicate that the smoke in Salt Lake City during SAMOZA had photochemically aged before reaching the urban area, thus originating from regional smoke rather than a local fire emission. Eight species included in this analysis (acetaldehyde, acetonitrile, benzene, C_8 aromatics, maleic anhydride, methanol, toluene, and formaldehyde) are on the EPA's list of HAPs, all shown in Figure 8. Their abundances were increased during smoke-influenced days by 45-217%. Those species had an average enhancement of 88% when smoke was present in Salt Lake City during SAMOZA. CO and $PM_{2.5}$, criteria air pollutants regulated by the EPA, also showed enhancement in smoke (88% and 174%, respectively), while ozone had a much lower increase at only 5%. Mixing ratios for all observed species during smoke-free and smoke-influenced days are found in Table S1. Solar radiation and temperature were additionally analyzed between the two groups, but because there was no statistically significant difference for either measurement ($1.58 \times 10^5 \pm 1.97 \times 10^5$ W/m^2 vs. $1.71 \times 10^5 \pm 2.07 \times 10^5$ W/m^2; 25 ± 5.6°C vs. 25 ± 6.3°C), they are not thought to contribute significantly to the changes in VOC concentration.

Figure S6 shows the total OH reactivity from VOCs increased by 50% during smoke-influenced days compared to smoke-free days (5.1 vs 3.4 s^{-1}). Terpenes including isoprene and monoterpenes that come largely from biogenic sources, are not as important during smoke-influenced periods due to formaldehyde and other oxygenated VOCs becoming more important contributors to OH reactivity during these days. Furanoid OH reactivity remained similar in both cases, which caused the contribution to total OH reactivity to decrease as aged fire smoke traveled to SLC during SAMOZA. Other VOC groups also show similar reactivity in both periods in spite of increased concentrations.

The impact of smoke on ozone production during SAMOZA was investigated in a separate publication, and thus is not a focus in this study. In brief, Ninneman et al. (2023) used observationally constrained photochemical box modeling for four case study days: including two smoke-free weekday and weekend days, and two smoke-influenced weekday and weekend days (Ninneman et al., 2023). We found that predicted levels of ozone were similar between the smoke-free and smoke-influenced days, however the sensitivity of ozone production was seen to be affected significantly by smoke. In both cases, ozone was not sensitive to reductions in NO_x without reductions of 75% or more. The difference was that ozone on smoke-free days was sensitive to VOCs in general, while ozone on smoke-influenced days was sensitive to fire VOCs to a much larger degree than any anthropogenic VOCs. While smoke did not cause a significant increase in ozone concentration during SAMOZA, smoke-emitted VOCs controlled the chemistry of ozone production when they reached the area. We refer to Ninneman et al (2023) for details of smoke impact on ozone, while in the next section, our analysis focuses on ozone photochemistry on smoke-free days which were the majority of the SAMOZA campaign.

3.4 Implications for Urban Photochemistry

Here we examine the transition of photochemistry in SLC during SAMOZA. We calculate the total OH reactivity (OHR) from NO_x ($tOHR_{NOx}$) and from VOCs ($tOHR_{VOC}$), and their ratio $\theta = tOHR_{NOx}/tOHR_{VOC}$ from SAMOZA measurements. The ratio θ was proposed as a metric to define the ozone production regime by Kirchner et al. (2001). By this metric, the production regime is VOC-limited when $\theta > 0.2$, NO_x-limited when $\theta < 0.01$, and transitional when θ is between 0.01 and 0.2. This metric has been applied in previous studies in the western US to show that VOCs emitted by smoke changed the ozone production regime in urban areas (Liang et al., 2022; Permar et al., 2023).

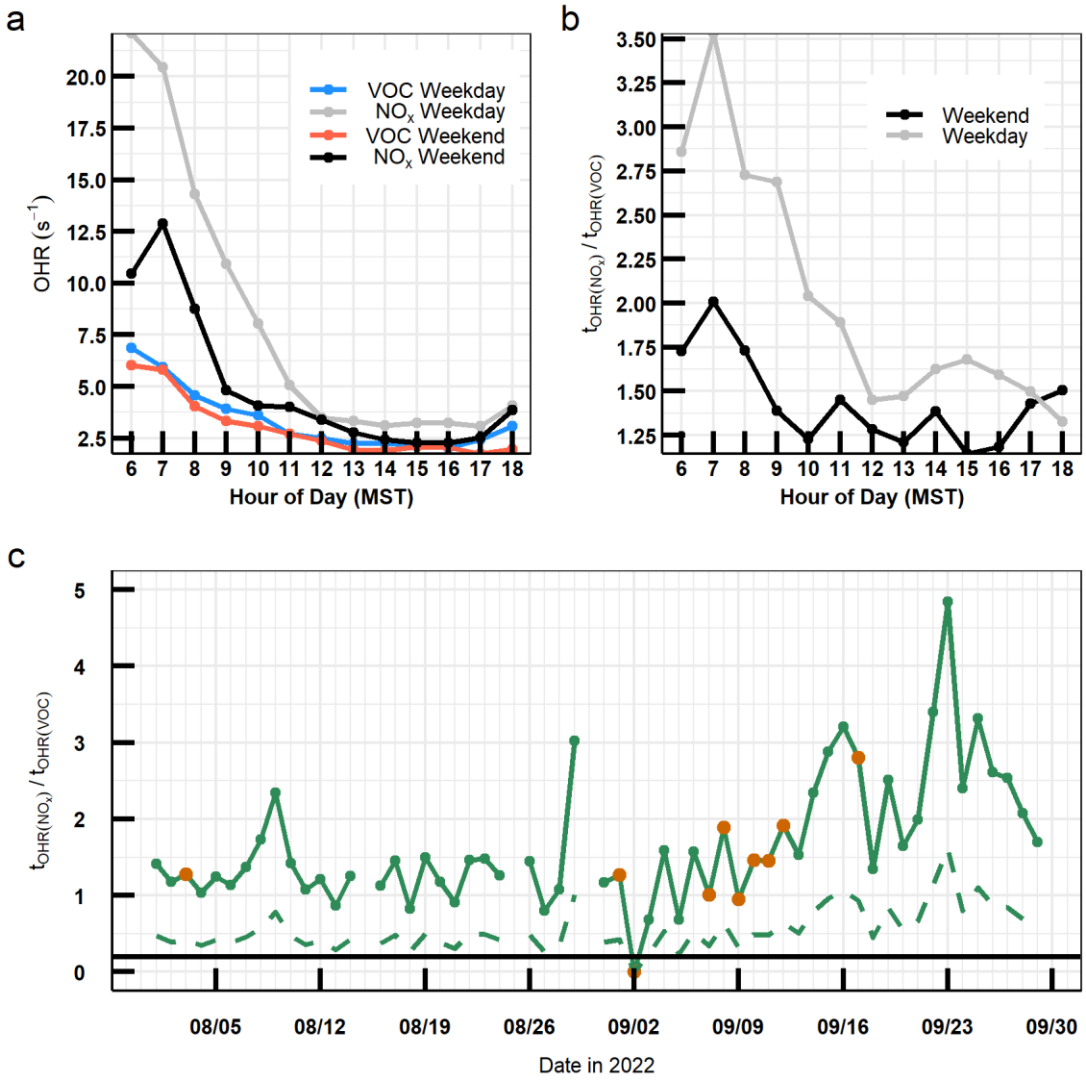

Figure 9. Daytime (06:00 – 18:00 MST) variations of OHR in s^{-1} a) for NO_x and VOCs differentiated by weekends and weekdays and b) for the ratio of $tOHR_{NOx}/tOHR_{VOC}$ or θ differentiated by weekends and weekdays. Both plots only include the 51 days not influenced by smoke. c) The daytime (06:00 – 18:00 MST) ratio of $tOHR_{NOx}/tOHR_{VOC}$ for each day during SAMOZA. Smoke-influenced days are highlighted in orange. The black horizontal line indicates where θ is equal to 0.2, the threshold between the VOC-limited and transitional regimes. The green dashed line shows the estimated lower bound of θ, by accounting for the potential influence from unmeasured VOCs; See text for details.

Figure 9 shows the daytime θ each day for the duration of SAMOZA, with smoke-influenced days highlighted in orange. θ was larger than 0.2 throughout the SAMOZA, and the ozone production is therefore estimated to have been VOC-limited. This is consistent with the findings of our modeling study (Ninneman et al., 2023). When separated by smoke-influenced and smoke-free days, there was little change in the regime, evident in the time series. On smoke-free days, θ averaged 1.8 ± 1.1, while on smoke-influenced days, θ averaged 1.4 ± 0.73, both

well above the threshold for the VOC-limited regime. This contrasts previous studies such as Liang et al. (2022) and Permar et al. (2023), which showed wildfire smoke lowering θ due to enhanced VOCs and shifting the ozone production regime from VOC-limited to a NO_x-limited or transitional regime. In the case of SAMOZA, NO_x concentrations were enhanced along with VOC concentrations during smoke-influenced days, which resulted in an increase in $tOHRNO_x$ from 4.71 s^{-1} on smoke-free days to 6.72 s^{-1} on smoke-influenced days. NO_x has been previously seen to have inconsistent enhancement during smoke events (Buysse et al., 2019).

The value of θ is seen to increase in the last weeks of the campaign driven by reduced $tOHR_{VOC}$. Figure S7 compares the VOC contribution to OH reactivity in the days before the air temperature in SLC dropped on September 9th, and those days after. $tOHR_{VOC}$ was lower in the period after the temperature dropped largely due to reduced biogenic terpenes and formaldehyde levels from decreased biological processes in the plants in and around SLC. In addition, formaldehyde also showed a decreased contribution to OH reactivity once the temperature dropped and its photochemical sources reduced due to the seasonal change, which is also captured in our PMF analysis. OH reactivity from NO_x did not have a change between the two time periods, being 2.2 s^{-1} before and after September 9th.

Figure 9 also shows the diurnal patterns of $tOHR_{VOC}$ and $tOHR_{NOx}$, separated by weekday versus weekend. $tOHR_{VOC}$ does not show an apparent weekday vs. weekend effect (Section 3.1). NO_x, on the other hand, shows greatly decreased OH reactivity on the weekend compared to the weekdays, likely because decreased traffic and commuters on the weekends led to lower NO_x emissions that have been widely reported in large urban areas including SLC (i.e., Kuprov et al., 2014; Valin et al., 2014). The diurnal patterns for the ratio θ of $tOHR_{NOx}/tOHR_{VOC}$ on weekends and weekdays are also plotted. The ratio θ was higher by a factor of 2 in the early daytime hours on weekdays, and larger by a factor of around 1 to 1.5 during afternoon hours, directly corresponding to the difference in $tOHR_{NOx}$ on weekends and weekdays. Future reduction of NO_x emissions will lower the θ thus moving the ozone chemistry to the transitional regime before NO_x-limited. However, based on SAMOZA data, that would require a significant NO_x emission reduction, supporting our modeling study based on the same measurements (Ninneman et al., 2023). Nevertheless, weekends in SLC would likely first show such photochemical regime changes under possible reduced future emissions.

One caveat of this analysis is the number of VOCs included in the calculation. We include 35 measured VOCs in SLC, while previous analyses such as Permar et al. (2023) reported that at least 154 VOCs are present in urban air (Boise, ID). Assuming the two cities have similar VOC composition, the results of Permar et al. (2023) would suggest that the 35 VOCs included here account for an estimated 60% of $tOHR_{VOC}$ for smoke-free urban air in that study, and roughly 55% of the $tOHR_{VOC}$ in smoke-impacted urban air. Therefore, adding other unreported VOCs in SLC would likely raise the value of $tOHR_{VOC}$ by a factor of 2-3 and thus lower θ by the same magnitude. This would not, however, be a great enough change to change the regime from VOC-limited to transitional or NO_x-limited. Such lower bound estimated θ remains above (though becoming closer to) 0.2 for each day of the campaign, shown in the dashed line in Figure 9. Further, we verify the robustness of the θ indicator for the ozone production regime by comparison to the ratio of formaldehyde to NO_2 concentration (FNR), proposed as an additional metric for use in urban areas (Sillman, 1995; Martin et al., 2004). The daily average of FNR is shown in Figure S8. This metric has previously been used in urban areas with the thresholds showing that ozone production is NO_x-limited when FNR>2, transitional when 1<FNR<2, and VOC-limited when FNR<1 (Duncan et al., 2010; Jin & Holloway, 2015; Li

et al., 2021). Most days indeed had FNR < 1, with decreasing values in the final weeks of the campaign and becoming more VOC-limited, broadly consistent with the θ metric. Nine days had FNR values between 1 and 2 and therefore showed a transitional regime, consistent with the lower bound estimated θ, though the exact thresholds of θ or FNR could be dependent on local chemical regimes and vary by cities (i.e., Jin et al., 2020; Souri et al., 2020) .

4 Conclusions

We present measurements of volatile organic compounds (VOCs) and other tracers taken in Salt Lake City, Utah in August-September of 2022 during the SAMOZA field campaign. 35 VOCs were measured with online PTR-ToF-MS and offline by DNPH cartridge samples that were subsequently analyzed by HPLC. The total measured VOCs in SLC averaged 32 ± 24 ppb, and the total calculated VOC OH reactivity averaged 3.7 ± 3.0 s^{-1}. Those VOCs with strong photochemical and biogenic sources such as formaldehyde and isoprene showed a 35-50% decrease in concentration after September 9th, 2022, when daily average air temperatures dropped by ~10°C in SLC. Diurnal patterns of most VOCs were typical of urban atmosphere, with high peak mixing ratios in the morning and increasing at night. Methanol and ethanol were the most abundant VOCs present. Terpenes were the largest contributors to OH reactivity in SLC. Contradicted to NO_x, we do not observe an apparent weekday vs. weekend effect in VOC abundance.

A PMF solution with 5 factors was used to further analyze VOC sources. Secondary and biogenic, traffic, and solvent uses (or VCPs) from personal care products and industrial sources were found to be important VOC sources in SLC during SAMOZA. Traffic and VCPs had roughly equivalent contributions to anthropogenic VOCs, in agreement with the 2020 NEI. Monoterpenes were found to have a more significant anthropogenic source than biogenic. Source tracer analysis showed high correlations between CO and aromatics, suggesting an important role in traffic emission, similar to the PMF results. Photochemical products like formaldehyde and biogenic VOCs like isoprene had two populations of correlation with CO, indicating some anthropogenic influence. The PMF analysis was used to find a semi-quantative estimate of the contributions to anthropogenic VOCs in SLC, however further measurements with spatial information are needed to provide more definitive answers.

10 out of 61 days during the SAMOZA field campaign were characterized as smoke-influenced. Smoke-free days showed lower abundances of most measured VOCs and thus lower OH reactivity from VOCs. Hazardous air pollutants (HAPs) and other VOCs increased by 45-217% due to the presence of aged smoke from regional wildfires during SAMOZA. The total OH reactivity of VOCs increased by 53% on smoke-influenced days, but the ozone production regime did not transition because of this increase likely due to an enhanced NO_x level during the same period.

The ozone photochemical regime was indicated using the ratio between total OH reactivity from NO_x and that from VOCs (or $\theta = tOHR_{NOx}/tOHR_{VOC}$). The chemical regime was found to be VOC-limited or close to the transitional regime throughout the campaign. The θ increased as temperatures dropped towards the end of the campaign due to the seasonal VOC reductions from biogenic emissions and photochemical sources. $tOHR_{NOx}$ was much higher on weekdays compared to weekends while $tOHR_{VOC}$ was similar between the two periods. These result in θ being a factor of 1-2 higher on weekdays compared to weekends, thus weekends in SLC may show the first observervations of any photochemical regime changes under possible reduced future emissions.

Acknowledgments

SAMOZA was funded by the Utah Division of Air Quality through a Science for Solutions grant. We want to thank all UDAQ personnel for their assistance during the experiment. We further acknowledge financial support from several industry partners including Rio Tinto Kennecott Utah Copper, LLC. Tesoro Refining and Marketing Co. Holly Frontier Woods Cross Refining LLC. Big West Oil LLC. Chevron USA Inc. The University of Montana group was also supported by the National Science Foundation (AGS # 2144896; EPSCoR # 2242802). We acknowledge Dr. Megan Willis at Colorado State University for assistance with additional VOC calibrations. The Utah Division of Air Quality had input on the project plan and reviewed a preliminary version of the final project report. The industry funders had no input on the experimental design, the final project report or any of the results presented in this manuscript.

Open Research

Final SAMOZA data has been archived and can be found at the University of Washington ResearchWorks archive: http://hdl.handle.net/1773/50049.

References

Abeleira, A., Pollack, I. B., Sive, B., Zhou, Y., Fischer, E. V., & Farmer, D. K. (2017). Source characterization of volatile organic compounds in the Colorado Northern Front Range Metropolitan Area during spring and summer 2015. Journal of Geophysical Research: Atmospheres, 122(6), 3595–3613. https://doi.org/10.1002/2016JD026227

Baasandorj, M., Brown, S., Hoch, S., Crosman, E., Long, R., Silva, P., et al. (2018). 2017 Utah Winter Fine Particulate Study Final Report. National Oceanic and Atmospheric Administration (NOAA). Retrieved from https://csl.noaa.gov/groups/csl7/measurements/2017uwfps/finalreport.pdf

Bhardwaj, N., Kelsch, A., Eatough, D. J., Thalman, R., Daher, N., Kelly, K., et al. (2021). Sources of Formaldehyde in Bountiful, Utah. Atmosphere, 12(3), 375. https://doi.org/10.3390/atmos12030375

821 Bierbach, A., Barnes, I., & Becker, K. H. (1995). Product and kinetic study of the oh-initiated
822 gas-phase oxidation of Furan, 2-methylfuran and furanaldehydes at ≈ 300 K. Atmospheric
823 Environment, 29(19), 2651–2660. https://doi.org/10.1016/1352-2310(95)00096-H
824 Bierbach, Arwid., Barnes, Ian., Becker, K. H., & Wiesen, Evelyn. (1994). Atmospheric
825 Chemistry of Unsaturated Carbonyls: Butenedial, 4-Oxo-2-pentenal, 3-Hexene-2,5-dione, Maleic
826 Anhydride, 3H-Furan-2-one, and 5-Methyl-3H-furan-2-one. Environmental Science &
827 Technology, 28(4), 715–729. https://doi.org/10.1021/es00053a028
828 Borbon, A., Dominutti, P., Panopoulou, A., Gros, V., Sauvage, S., Farhat, M., et al. (2023).
829 Ubiquity of Anthropogenic Terpenoids in Cities Worldwide: Emission Ratios, Emission
830 Quantification and Implications for Urban Atmospheric Chemistry. Journal of Geophysical
831 Research: Atmospheres, 128(7), e2022JD037566. https://doi.org/10.1029/2022JD037566
832 Bryant, D. J., Nelson, B. S., Swift, S. J., Budisulistiorini, S. H., Drysdale, W. S., Vaughan, A. R.,
833 et al. (2023). Biogenic and anthropogenic sources of isoprene and monoterpenes and their
834 secondary organic aerosol in Delhi, India. Atmospheric Chemistry and Physics, 23(1), 61–83.
835 https://doi.org/10.5194/acp-23-61-2023
836 Buysse, C. E., Kaulfus, A., Nair, U., & Jaffe, D. A. (2019). Relationships between Particulate
837 Matter, Ozone, and Nitrogen Oxides during Urban Smoke Events in the Western US.
838 Environmental Science & Technology, 53(21), 12519–12528.
839 https://doi.org/10.1021/acs.est.9b05241
840 Churkina, G., Kuik, F., Bonn, B., Lauer, A., Grote, R., Tomiak, K., & Butler, T. M. (2017).
841 Effect of VOC Emissions from Vegetation on Air Quality in Berlin during a Heatwave.
842 Environmental Science and Technology, 51(11), 6120–6130.
843 https://doi.org/10.1021/acs.est.6b06514

844 Coggon, M. M., McDonald, B. C., Vlasenko, A., Veres, P. R., Bernard, F., Koss, A. R., et al.
845 (2018). Diurnal Variability and Emission Pattern of Decamethylcyclopentasiloxane (D_5) from
846 the Application of Personal Care Products in Two North American Cities. Environmental
847 Science & Technology, 52(10), 5610–5618. https://doi.org/10.1021/acs.est.8b00506
848 Coggon, M. M., Gkatzelis, G. I., McDonald, B. C., Gilman, J. B., Schwantes, R. H., Abuhassan,
849 N., et al. (2021). Volatile chemical product emissions enhance ozone and modulate urban
850 chemistry. Proceedings of the National Academy of Sciences, 118(32), e2026653118.
851 https://doi.org/10.1073/pnas.2026653118
852 Coggon, M. M., Stockwell, C. E., Claflin, M. S., Pfannerstill, E. Y., Lu, X., Gilman, J. B., et al.
853 (2023). Identifying and correcting interferences to PTR-ToF-MS measurements of isoprene and
854 other urban volatile organic compounds (preprint). Gases/In Situ Measurement/Instruments and
855 Platforms. https://doi.org/10.5194/egusphere-2023-1497
856 De Gouw, J. A., Middlebrook, A. M., Warneke, C., Goldan, P. D., Kuster, W. C., Roberts, J. M.,
857 et al. (2005). Budget of organic carbon in a polluted atmosphere: Results from the New England
858 Air Quality Study in 2002. Journal of Geophysical Research: Atmospheres, 110(D16),
859 2004JD005623. https://doi.org/10.1029/2004JD005623
860 De Gouw, J. A., Gilman, J. B., Kim, S. -W., Lerner, B. M., Isaacman-VanWertz, G., McDonald,
861 B. C., et al. (2017). Chemistry of Volatile Organic Compounds in the Los Angeles basin:
862 Nighttime Removal of Alkenes and Determination of Emission Ratios. Journal of Geophysical
863 Research: Atmospheres, 122(21). https://doi.org/10.1002/2017JD027459
864 Dreessen, J., Sullivan, J., & Delgado, R. (2016). Observations and impacts of transported
865 Canadian wildfire smoke on ozone and aerosol air quality in the Maryland region on June 9–12,

2015. Journal of the Air and Waste Management Association, 66(9), 842–862. https://doi.org/10.1080/10962247.2016.1161674

Duncan, B. N., Yoshida, Y., Olson, J. R., Sillman, S., Martin, R. V., Lamsal, L., et al. (2010). Application of OMI observations to a space-based indicator of NO_x and VOC controls on surface ozone formation. Atmospheric Environment, 44(18), 2213–2223. https://doi.org/10.1016/j.atmosenv.2010.03.010

Felzer, B. S., Cronin, T., Reilly, J. M., Melillo, J. M., & Wang, X. (2007). Impacts of ozone on trees and crops. Comptes Rendus Geoscience, 339(11–12), 784–798. https://doi.org/10.1016/j.crte.2007.08.008

Folberth, G. A., Hauglustaine, D. A., Lathière, J., & Brocheton, F. (2006). Interactive chemistry in the Laboratoire de Météorologie Dynamique general circulation model: model description and impact analysis of biogenic hydrocarbons on tropospheric chemistry. Atmospheric Chemistry and Physics, 6(8), 2273–2319. https://doi.org/10.5194/acp-6-2273-2006

Gilman, J. B., Lerner, B. M., Kuster, W. C., & Gouw, J. A. D. (2013). Source signature of volatile organic compounds from oil and natural gas operations in northeastern Colorado. Environmental Science and Technology, 47(3), 1297–1305. https://doi.org/10.1021/es304119a

Gilman, J. B., Lerner, B. M., Kuster, W. C., Goldan, P. D., Warneke, C., Veres, P. R., et al. (2015). Biomass burning emissions and potential air quality impacts of volatile organic compounds and other trace gases from fuels common in the US. Atmospheric Chemistry and Physics, 15(24), 13915–13938. https://doi.org/10.5194/acp-15-13915-2015

Gilman, Jessica B., Kuster, W. C., Goldan, P. D., Herndon, S. C., Zahniser, M. S., Tucker, S. C., et al. (2009). Measurements of volatile organic compounds during the 2006 TexAQS/GoMACCS campaign: Industrial influences, regional characteristics, and diurnal

889 dependencies of the OH reactivity. Journal of Geophysical Research, 114, D00F06.
890 https://doi.org/10.1029/2008JD011525
891 Gkatzelis, G. I., Coggon, M. M., McDonald, B. C., Peischl, J., Aikin, K. C., Gilman, J. B., et al.
892 (2021). Identifying Volatile Chemical Product Tracer Compounds in U.S. Cities. Environmental
893 Science and Technology, 55(1), 188–199. https://doi.org/10.1021/acs.est.0c05467
894 Gkatzelis, G. I., Coggon, M. M., McDonald, B. C., Peischl, J., Gilman, J. B., Aikin, K. C., et al.
895 (2021). Observations Confirm that Volatile Chemical Products Are a Major Source of
896 Petrochemical Emissions in U.S. Cities. Environmental Science & Technology, 55(8), 4332–
897 4343. https://doi.org/10.1021/acs.est.0c05471
898 Gong, X., Kaulfus, A., Nair, U., & Jaffe, D. A. (2017). Quantifying O_3 Impacts in Urban Areas
899 Due to Wildfires Using a Generalized Additive Model. Environmental Science & Technology,
900 51(22), 13216–13223. https://doi.org/10.1021/acs.est.7b03130
901 Gu, S., Guenther, A., & Faiola, C. (2021). Effects of Anthropogenic and Biogenic Volatile
902 Organic Compounds on Los Angeles Air Quality. Environmental Science & Technology, 55(18),
903 12191–12201. https://doi.org/10.1021/acs.est.1c01481
904 Guenther, A. B., Jiang, X., Heald, C. L., Sakulyanontvittaya, T., Duhl, T., Emmons, L. K., &
905 Wang, X. (2012). The Model of Emissions of Gases and Aerosols from Nature version 2.1
906 (MEGAN2.1): an extended and updated framework for modeling biogenic emissions.
907 Geoscientific Model Development, 5(6), 1471–1492. https://doi.org/10.5194/gmd-5-1471-2012
908 Hansen, R. F., Griffith, S. M., Dusanter, S., Gilman, J. B., Graus, M., Kuster, W. C., et al.
909 (2021). Measurements of Total OH Reactivity During CalNex-LA. Journal of Geophysical
910 Research: Atmospheres, 126(11), e2020JD032988. https://doi.org/10.1029/2020JD032988

911 Horel, J., Crosman, E., Jacques, A., Blaylock, B., Arens, S., Long, A., et al. (2016). Summer
912 ozone concentrations in the vicinity of the Great Salt Lake. Atmospheric Science Letters, 17(9),
913 480–486. https://doi.org/10.1002/asl.680
914 Hu, L., Millet, D. B., Baasandorj, M., Griffis, T. J., Travis, K. R., Tessum, C. W., et al. (2015a).
915 Emissions of C 6 –C 8 aromatic compounds in the United States: Constraints from tall tower and
916 aircraft measurements. Journal of Geophysical Research: Atmospheres, 120(2), 826–842.
917 https://doi.org/10.1002/2014JD022627
918 Hu, L., Millet, D. B., Mohr, M. J., Wells, K. C., Griffis, T. J., & Helmig, D. (2011). Sources and
919 seasonality of atmospheric methanol based on tall tower measurements in the US Upper
920 Midwest. Atmospheric Chemistry and Physics, 11(21), 11145–11156.
921 https://doi.org/10.5194/acp-11-11145-2011
922 Hu, Lu, Millet, D. B., Baasandorj, M., Griffis, T. J., Turner, P., Helmig, D., et al. (2015b).
923 Isoprene emissions and impacts over an ecological transition region in the U.S. Upper Midwest
924 inferred from tall tower measurements. Journal of Geophysical Research: Atmospheres, 120(8),
925 3553–3571. https://doi.org/10.1002/2014JD022732
926 Huangfu, Y., Yuan, B., Wang, S., Wu, C., He, X., Qi, J., et al. (2021). Revisiting Acetonitrile as
927 Tracer of Biomass Burning in Anthropogenic-Influenced Environments. Geophysical Research
928 Letters, 48(11). https://doi.org/10.1029/2020GL092322
929 Jaffe, D. A., Wigder, N., Downey, N., Pfister, G., Boynard, A., & Reid, S. B. (2013). Impact of
930 wildfires on ozone exceptional events in the western U.S. Environmental Science and
931 Technology, 47(19), 11065–11072. https://doi.org/10.1021/es402164f
932 Jaffe, D. A., Cooper, O. R., Fiore, A. M., Henderson, B. H., Tonnesen, G. S., Russell, A. G., et
933 al. (2018). Scientific assessment of background ozone over the U.S.: Implications for air quality

management. Elementa: Science of the Anthropocene, 6, 56.
https://doi.org/10.1525/elementa.309

Jaffe, D. A., O'Neill, S. M., Larkin, N. K., Holder, A. L., Peterson, D. L., Halofsky, J. E., & Rappold, A. G. (2020). Wildfire and prescribed burning impacts on air quality in the United States. Journal of the Air & Waste Management Association, 70(6), 583–615. https://doi.org/10.1080/10962247.2020.1749731

Jaffe, D. A., Ninneman, M., & Chan, H. C. (2022). NO_x and O_3 Trends at U.S. Non-Attainment Areas for 1995–2020: Influence of COVID-19 Reductions and Wildland Fires on Policy-Relevant Concentrations. Journal of Geophysical Research: Atmospheres, 127(11). https://doi.org/10.1029/2021JD036385

Jaffe, D. A., Ninneman, M., Nguyen, L., Lee, H., Hu, L., Ketcherside, D., et al. (2024). Key results from the salt lake regional smoke, ozone, and aerosol study (SAMOZA). Journal of the Air & Waste Management Association, 1–18. https://doi.org/10.1080/10962247.2024.2301956

Jin, L., Permar, W., Selimovic, V., Ketcherside, D., Yokelson, R. J., Hornbrook, R. S., et al. (2023). Constraining emissions of volatile organic compounds from western US wildfires with WE-CAN and FIREX-AQ airborne observations. Atmospheric Chemistry and Physics, 23(10), 5969–5991. https://doi.org/10.5194/acp-23-5969-2023

Jin, X., & Holloway, T. (2015). Spatial and temporal variability of ozone sensitivity over China observed from the Ozone Monitoring Instrument. Journal of Geophysical Research: Atmospheres, 120(14), 7229–7246. https://doi.org/10.1002/2015JD023250

Jin, X., Fiore, A., Boersma, K. F., Smedt, I. D., & Valin, L. (2020). Inferring Changes in Summertime Surface Ozone–NO_x–VOC Chemistry over U.S. Urban Areas from Two Decades

of Satellite and Ground-Based Observations. Environmental Science & Technology, 54(11), 6518–6529. https://doi.org/10.1021/acs.est.9b07785

Kalbande, R., Yadav, R., Maji, S., Rathore, D. S., & Beig, G. (2022). Characteristics of VOCs and their contribution to O_3 and SOA formation across seasons over a metropolitan region in India. Atmospheric Pollution Research, 13(8), 101515. https://doi.org/10.1016/j.apr.2022.101515

Khan, M., Schlich, B.-L., Jenkin, M., Shallcross, B., Moseley, K., Walker, C., et al. (2018). A Two-Decade Anthropogenic and Biogenic Isoprene Emissions Study in a London Urban Background and a London Urban Traffic Site. Atmosphere, 9(10), 387. https://doi.org/10.3390/atmos9100387

Kirchner, F., Jeanneret, F., Clappier, A., Krüger, B., Van Den Bergh, H., & Calpini, B. (2001). Total VOC reactivity in the planetary boundary layer: 2. A new indicator for determining the sensitivity of the ozone production to VOC and NO_x. Journal of Geophysical Research: Atmospheres, 106(D3), 3095–3110. https://doi.org/10.1029/2000JD900603

Kuprov, R., Eatough, D. J., Cruickshank, T., Olson, N., Cropper, P. M., & Hansen, J. C. (2014). Composition and secondary formation of fine particulate matter in the Salt Lake Valley: Winter 2009. Journal of the Air & Waste Management Association, 64(8), 957–969. https://doi.org/10.1080/10962247.2014.903878

Lee, H., & Jaffe, D. A. (2024). Impact of wildfire smoke on ozone concentrations using a Generalized Additive model in Salt Lake City, Utah, USA, 2006–2022. Journal of the Air & Waste Management Association, 74(2), 116–130. https://doi.org/10.1080/10962247.2023.2291197

Li, D., Wang, S., Xue, R., Zhu, J., Zhang, S., Sun, Z., & Zhou, B. (2021). OMI-observed HCHO in Shanghai, China, during 2010–2019 and ozone sensitivity inferred by an improved HCHO／

NO_2 ratio. Atmospheric Chemistry and Physics, 21(20), 15447–15460. https://doi.org/10.5194/acp-21-15447-2021

Li, X.-B., Yuan, B., Wang, S., Wang, C., Lan, J., Liu, Z., et al. (2022). Variations and sources of volatile organic compounds (VOCs) in urban region: insights from measurements on a tall tower. Atmospheric Chemistry and Physics, 22(16), 10567–10587. https://doi.org/10.5194/acp-22-10567-2022

Liang, Y., Weber, R. J., Misztal, P. K., Jen, C. N., & Goldstein, A. H. (2022). Aging of Volatile Organic Compounds in October 2017 Northern California Wildfire Plumes. Environmental Science and Technology, 56(3), 1557–1567. https://doi.org/10.1021/acs.est.1c05684

Lill, E., Lindaas, J., Juncosa Calahorrano, J. F., Campos, T., Flocke, F., Apel, E. C., et al. (2022). Wildfire-driven changes in the abundance of gas-phase pollutants in the city of Boise, ID during summer 2018. Atmospheric Pollution Research, 13(1), 101269. https://doi.org/10.1016/j.apr.2021.101269

Liu, X., Huey, L. G., Yokelson, R. J., Selimovic, V., Simpson, I. J., Müller, M., et al. (2017). Airborne measurements of western U.S. wildfire emissions: Comparison with prescribed burning and air quality implications. Journal of Geophysical Research, 122(11), 6108–6129. https://doi.org/10.1002/2016JD026315

Ma, M., Gao, Y., Ding, A., Su, H., Liao, H., Wang, S., et al. (2022). Development and Assessment of a High-Resolution Biogenic Emission Inventory from Urban Green Spaces in China. Environmental Science and Technology, 56(1), 175–184. https://doi.org/10.1021/acs.est.1c06170

MacDonald, R. C., & Fall, R. (1993). Detection of substantial emissions of methanol from plants to the atmosphere. Atmospheric Environment. Part A. General Topics, 27(11), 1709–1713. https://doi.org/10.1016/0960-1686(93)90233-O

Martin, R. V., Fiore, A. M., & Van Donkelaar, A. (2004). Space-based diagnosis of surface ozone sensitivity to anthropogenic emissions. Geophysical Research Letters, 31(6), 2004GL019416. https://doi.org/10.1029/2004GL019416

McDonald, B. C., De Gouw, J. A., Gilman, J. B., Jathar, S. H., Akherati, A., Cappa, C. D., et al. (2018). Volatile chemical products emerging as largest petrochemical source of urban organic emissions. Science, 359(6377), 760–764. https://doi.org/10.1126/science.aaq0524

Millet, D. B., Apel, E., Henze, D. K., Hill, J., Marshall, J. D., Singh, H. B., & Tessum, C. W. (2012). Natural and Anthropogenic Ethanol Sources in North America and Potential Atmospheric Impacts of Ethanol Fuel Use. Environmental Science & Technology, 46(15), 8484–8492. https://doi.org/10.1021/es300162u

Millet, D. B., Baasandorj, M., Hu, L., Mitroo, D., Turner, J., & Williams, B. J. (2016). Nighttime Chemistry and Morning Isoprene Can Drive Urban Ozone Downwind of a Major Deciduous Forest. Environmental Science & Technology, 50(8), 4335–4342. https://doi.org/10.1021/acs.est.5b06367

Mouat, A. P., Paton-Walsh, C., Simmons, J. B., Ramirez-Gamboa, J., Griffith, D. W. T., & Kaiser, J. (2022). Measurement report: Observations of long-lived volatile organic compounds from the 2019–2020 Australian wildfires during the COALA campaign. Atmospheric Chemistry and Physics, 22(17), 11033–11047. https://doi.org/10.5194/acp-22-11033-2022

Müller, M., Anderson, B. E., Beyersdorf, A. J., Crawford, J. H., Diskin, G. S., Eichler, P., et al. (2016). In situ measurements and modeling of reactive trace gases in a small biomass burning

plume. Atmospheric Chemistry and Physics, 16(6), 3813–3824. https://doi.org/10.5194/acp-16-3813-2016

National Research Council (NRC). (1991). Rethinking the Ozone Problem in Urban and Regional Air Pollution. Washington, D.C.: National Academy Press.

Ninneman, M., Lyman, S., Hu, L., Cope, E., Ketcherside, D., & Jaffe, D. (2023). Investigation of Ozone Formation Chemistry during the Salt Lake Regional Smoke, Ozone, and Aerosol Study (SAMOZA). ACS Earth and Space Chemistry, 7(12), 2521–2534. https://doi.org/10.1021/acsearthspacechem.3c00235

Norris, G., Duvall, R., Brown, S., & Bai, S. (2014). EPA Positive Matrix Factorization (PMF) 5.0 Fundamentals and User Guide. Retrieved from https://www.epa.gov/sites/default/files/2015-02/documents/pmf_5.0_user_guide.pdf

Nuvolone, D., Petri, D., & Voller, F. (2018). The effects of ozone on human health. Environmental Science and Pollution Research, 25(9), 8074–8088. https://doi.org/10.1007/s11356-017-9239-3

Paatero, P., & Tapper, U. (1994). Positive matrix factorization: A non-negative factor model with optimal utilization of error estimates of data values. Environmetrics, 5(2), 111–126. https://doi.org/10.1002/env.3170050203

Peng, Y., Mouat, A. P., Hu, Y., Li, M., McDonald, B. C., & Kaiser, J. (2022). Source appointment of volatile organic compounds and evaluation of anthropogenic monoterpene emission estimates in Atlanta, Georgia. Atmospheric Environment, 288, 119324. https://doi.org/10.1016/j.atmosenv.2022.119324

Permar, W., Wang, Q., Selimovic, V., Wielgasz, C., Yokelson, R. J., Hornbrook, R. S., et al. (2021). Emissions of Trace Organic Gases From Western U.S. Wildfires Based on WE-CAN

Aircraft Measurements. Journal of Geophysical Research: Atmospheres, 126(11). https://doi.org/10.1029/2020JD033838

Permar, W., Jin, L., Peng, Q., O'Dell, K., Lill, E., Selimovic, V., et al. (2023). Atmospheric OH reactivity in the western United States determined from comprehensive gas-phase measurements during WE-CAN. Environmental Science: Atmospheres, 3(1), 97–114. https://doi.org/10.1039/D2EA00063F

Rickly, P. S., Coggon, M. M., Aikin, K. C., Alvarez, R. J., Baidar, S., Gilman, J. B., et al. (2023). Influence of Wildfire on Urban Ozone: An Observationally Constrained Box Modeling Study at a Site in the Colorado Front Range. Environmental Science & Technology. https://doi.org/10.1021/acs.est.2c06157

Ring, A. M., Dickerson, R. R., Sebol, A. E., Ren, X., Benish, S. E., Salawitch, R. J., et al. (2023). Anthropogenic VOCs in the Long Island Sound, NY Airshed and their role in ozone production. Atmospheric Environment, 296, 119583. https://doi.org/10.1016/j.atmosenv.2023.119583

Sakulyanontvittaya, T., Duhl, T., Wiedinmyer, C., Helmig, D., Matsunaga, S., Potosnak, M., et al. (2008). Monoterpene and Sesquiterpene Emission Estimates for the United States. Environmental Science & Technology, 42(5), 1623–1629. https://doi.org/10.1021/es702274e

Salisbury, G., Williams, J., Holzinger, R., Gros, V., Mihalopoulos, N., Vrekoussis, M., et al. (2003). Ground-based PTR-MS measurements of reactive organic compounds during the MINOS campaign in Crete, July–August 2001. Atmospheric Chemistry and Physics, 3(4), 925–940. https://doi.org/10.5194/acp-3-925-2003

Sanchez, D., Seco, R., Gu, D., Guenther, A., Mak, J., Lee, Y., et al. (2021). Contributions to OH reactivity from unexplored volatile organic compounds measured by PTR-ToF-MS – a case study in a suburban forest of the Seoul metropolitan area during the Korea–United States Air

Quality Study (KORUS-AQ) 2016. Atmospheric Chemistry and Physics, 21(8), 6331–6345. https://doi.org/10.5194/acp-21-6331-2021

Sekimoto, K., Li, S.-M., Yuan, B., Koss, A., Coggon, M., Warneke, C., & De Gouw, J. (2017). Calculation of the sensitivity of proton-transfer-reaction mass spectrometry (PTR-MS) for organic trace gases using molecular properties. International Journal of Mass Spectrometry, 421, 71–94. https://doi.org/10.1016/j.ijms.2017.04.006

Sekimoto, K., Koss, A. R., Gilman, J. B., Selimovic, V., Coggon, M. M., Zarzana, K. J., et al. (2018). High-and low-temperature pyrolysis profiles describe volatile organic compound emissions from western US wildfire fuels. Atmospheric Chemistry and Physics, 18(13), 9263–9281. https://doi.org/10.5194/acp-18-9263-2018

Selimovic, V., Ketcherside, D., Chaliyakunnel, S., Wielgasz, C., Permar, W., Angot, H., et al. (2022). Atmospheric biogenic volatile organic compounds in the Alaskan Arctic tundra: constraints from measurements at Toolik Field Station (preprint). Gases/Field Measurements/Troposphere/Chemistry (chemical composition and reactions). https://doi.org/10.5194/acp-2022-396

Seltzer, K. M., Pennington, E., Rao, V., Murphy, B. N., Strum, M., Isaacs, K. K., & Pye, H. O. T. (2021). Reactive organic carbon emissions from volatile chemical products. Atmospheric Chemistry and Physics, 21(6), 5079–5100. https://doi.org/10.5194/acp-21-5079-2021

Shrestha, S., Yoon, S., Erickson, M. H., Guo, F., Mehra, M., Bui, A. A. T., et al. (2022). Traffic, transport, and vegetation drive VOC concentrations in a major urban area in Texas. Science of The Total Environment, 838, 155861. https://doi.org/10.1016/j.scitotenv.2022.155861

1090 Sillman, S. (1995). The use of NO_y, H_2O_2 , and HNO_3 as indicators for ozone-NO_x-hydrocarbon
1091 sensitivity in urban locations. Journal of Geophysical Research: Atmospheres, 100(D7), 14175–
1092 14188. https://doi.org/10.1029/94JD02953
1093 Simon, L., Gros, V., Petit, J.-E., Truong, F., Sarda-Estève, R., Kalalian, C., et al. (2023). Two
1094 years of volatile organic compound online in situ measurements at the Site Instrumental de
1095 Recherche par Télédétection Atmosphérique (Paris region, France) using proton-transfer-
1096 reaction mass spectrometry. Earth System Science Data, 15(5), 1947–1968.
1097 https://doi.org/10.5194/essd-15-1947-2023
1098 Souri, A. H., Nowlan, C. R., Wolfe, G. M., Lamsal, L. N., Chan Miller, C. E., Abad, G. G., et al.
1099 (2020). Revisiting the effectiveness of HCHO/NO2 ratios for inferring ozone sensitivity to its
1100 precursors using high resolution airborne remote sensing observations in a high ozone episode
1101 during the KORUS-AQ campaign. Atmospheric Environment, 224, 117341.
1102 https://doi.org/10.1016/j.atmosenv.2020.117341
1103 Stroud, C. A., Morneau, G., Makar, P. A., Moran, M. D., Gong, W., Pabla, B., et al. (2008). OH-
1104 reactivity of volatile organic compounds at urban and rural sites across Canada: Evaluation of air
1105 quality model predictions using speciated VOC measurements. Atmospheric Environment,
1106 42(33), 7746–7756. https://doi.org/10.1016/j.atmosenv.2008.05.054
1107 Ulbrich, I. M., Canagaratna, M. R., Zhang, Q., Worsnop, D. R., & Jimenez, J. L. (2009).
1108 Interpretation of organic components from Positive Matrix Factorization of aerosol mass
1109 spectrometric data. Atmospheric Chemistry and Physics, 9(9), 2891–2918.
1110 https://doi.org/10.5194/acp-9-2891-2009
1111 Utah DAQ. (2022). Division of Air Quality Annual Monitoring Network Plan 2022. Retrieved
1112 from https://documents.deq.utah.gov/air-quality/planning/air-monitoring/DAQ-2022-007189.pdf

1113 Valin, L. C., Russell, A. R., & Cohen, R. C. (2014). Chemical feedback effects on the spatial
1114 patterns of the NOx weekend effect: a sensitivity analysis. Atmospheric Chemistry and Physics,
1115 14(1), 1–9. https://doi.org/10.5194/acp-14-1-2014
1116 Wagner, P., & Kuttler, W. (2014). Biogenic and anthropogenic isoprene in the near-surface
1117 urban atmosphere — A case study in Essen, Germany. Science of The Total Environment, 475,
1118 104–115. https://doi.org/10.1016/j.scitotenv.2013.12.026
1119 Warneke, C., Gouw, J. A. D., Holloway, J. S., Peischl, J., Ryerson, T. B., Atlas, E., et al. (2012).
1120 Multiyear trends in volatile organic compounds in Los Angeles, California: Five decades of
1121 decreasing emissions. Journal of Geophysical Research Atmospheres, 117(17).
1122 https://doi.org/10.1029/2012JD017899
1123 Womack, C. C., McDuffie, E. E., Edwards, P. M., Bares, R., De Gouw, J. A., Docherty, K. S., et
1124 al. (2019). An Odd Oxygen Framework for Wintertime Ammonium Nitrate Aerosol Pollution in
1125 Urban Areas: NO_x and VOC Control as Mitigation Strategies. Geophysical Research Letters,
1126 46(9), 4971–4979. https://doi.org/10.1029/2019GL082028
1127 Xu, S., Chen, M., Feng, T., Zhan, L., Zhou, L., & Yu, G. (2021). Use ggbreak to Effectively
1128 Utilize Plotting Space to Deal With Large Datasets and Outliers. Frontiers in Genetics, 12,
1129 774846. https://doi.org/10.3389/fgene.2021.774846
1130 Zhang, Z., Zhang, Y., Wang, X., Lü, S., Huang, Z., Huang, X., et al. (2016). Spatiotemporal
1131 patterns and source implications of aromatic hydrocarbons at six rural sites across China's
1132 developed coastal regions: AROMATICS IN CHINA'S DEVELOPED REGIONS. Journal of
1133 Geophysical Research: Atmospheres, 121(11), 6669–6687.
1134 https://doi.org/10.1002/2016JD025115